# Response Surface Methodology (RSM) Optimization of Geopolymer Palm Oil Clinker Fines (GeoPOCF) and Bitumen Content for Geopolymer Modified Asphalt Mixtures

by

Mohamad Rahmad Bin Alias
18002887

Dissertation submitted in partial fulfilment of
the requirements for
Bachelor of Civil Engineering with Honours

JANUARY 2022

Universiti Teknologi PETRONAS
Bandar Seri Iskandar
32610
Perak Darul Ridzuan

# CERTIFICATION OF APPROVAL

**Response Surface Methodology (RSM) Optimization of Geopolymer Palm Oil Clinker Fines (GeoPOCF) and Bitumen Content for Geopolymer Modified Asphalt Mixtures**

By

Mohamad Rahmad Bin Alias
18002887

A project dissertation submitted to the

Civil Engineering Programme

Universiti Teknologi PETRONAS

in partial fulfilment of the requirement for the

BACHELOR OF CIVIL ENGINEERING WITH HONOURS

Approved by,

(Ir. Dr Muslich Hartadi Sutanto)

UNIVERSITI TEKNOLOGI PETRONAS

SERI ISKANDAR, PERAK

January 2022

# CERTIFICATION OF ORIGINALITY

This is to certify that I am responsible for the work submitted in this project, that the original work is my own except as specified in the references and acknowledgements, and that the original work contained herein have not been undertaken or done by unspecified sources or persons.

MOHAMAD RAHMAD BIN ALIAS

# ABSTRACT

Cracking and rutting of the road surface have been identified as the most prevalent concerns in Malaysia. It is especially concerning because Malaysia's roads contribute significantly to its economic growth. The poor asphalt mixtures in the pavement structure were widely identified as the cause of road problems. This study is to develop models for geopolymer palm oil clinker fines (GeoPOCF) asphalt mixtures at varying content of GeoPOCF and bitumen and producing output reponses in terms of volumetric and Marshall mix design properties, which are bulk unit weight (BUW), air voids, Marshall stability and Marshall flow using response surface methodology (RSM) software and to characterize the GeoPOCF powder, unmodified bitumen and GeoPOCF modified bitumen (GeoPOCF-MB). The RSM software was utilized to determine the optimum content of GeoPOCF and bitumen. A quadratic regression model with a p-value < 5% for all responses at the globalize optimum conditions was obtained using the central composite design (CCD) process in RSM software. ANOVA analysis shows that GeoPOCF content significantly impacts asphalt mixtures characteristics. After optimization, the optimum GeoPOCF content is 6.15%, and bitumen content is 4.85%. The percentage error between the RSM predicted, and laboratory results are < 5% for all responses when using the optimum GeoPOCF and bitumen content. The bitumen modification produces stiffer asphalt mixtures, causing higher Marshall stability and BUW while having values within range for air voids and Marshall flow according to JKR standards. Lastly, the characterization of the GeoPOCF-MB was assessed via X-Ray Diffraction (XRD), Fourier Transform Infrared Spectroscopy (FTIR) and Scanning Electron Microscope/Energy Dispersive X-Ray (SEM/EDX). The characterization results demonstrate that GeoPOCF has a substantial impact on the characteristics of bitumen. In addition, GeoPOCF has a lot of potential as an alternative bitumen modifier to increase sustainability, according to the study's findings.

# ACKNOWLEDGEMENT

Alhamdulillah, all praises to Allah's grace and permission, I was able to finish my final year project for two semesters in a row. Even amid the Covid-19 epidemic, which has hampered learning and research activities.

I want to express my sincere gratitude to Ir Dr Muslich Hartadi Sutanto, who served as a supervisor during the project and provided invaluable direction, expertise, and experience. I am delighted to have him as my supervisor since he constantly encourages me to finish the research.

In addition, a big thank you to Mr Nura Shehu Aliyu Yaro, who worked as an assistant to my supervisor and assisted me throughout the project.

I would also like to take this opportunity to thank all of the Civil Engineering members for their assistance and consideration. Thank you very much to both Final Year Project Coordinators for providing project guidelines and my other Final Year friends with information and help whenever I needed it.

Thank you, my parent and family, for their unending support, encouragement, inspiration, and attention. Special thanks to all of my friends who have supported me during the study's setbacks.

Finally, I would like to express my appreciation to everyone who has contributed to this project, whether directly or indirectly.

# Table of Contents


**CERTIFICATION OF APPROVAL** ........ i

**CERTIFICATION OF ORIGINALITY** ........ ii

**ABSTRACT** ........ iii

**ACKNOWLEDGEMENT** ........ iv

**Table of Contents** ........ v

**List of Figures** ........ vii

**List of Tables** ........ viii

**CHAPTER 1** ........ 1

**INTRODUCTION** ........ 1

**1.1 Background of Study** ........ 1

**1.2 Problem Statement** ........ 4

**1.3 Objectives of Study** ........ 5

**1.4 Scope of Study** ........ 5

**CHAPTER 2** ........ 7

**LITERATURE REVIEW AND THEORIES** ........ 7

**2.1 Geopolymer Palm Oil Clinker Fines (GeoPOCF)** ........ 7

**2.2 Volumetric Parameters and Marshall Properties** ........ 8

**2.3 Marshall Mix Design** ........ 9

**2.4 Response Surface Methodology (RSM)** ........ 11

**2.5 XRD, FTIR and SEM/EDX Analysis** ........ 12

**CHAPTER 3** ........ 19

**METHODOLOGY** ........ 19

**3.1 Project Workflow** ........ 19

**3.1.1 Laboratory Experiment and Data Collection** ........ 20

**3.1.2 Software Analysis and Modelling** ........ 23

**3.1.3 GeoPOCF and GeoPOCF-MB Characterization** ........ 25

**3.1.4 Analysis and Discussion of Findings** ........ 26

**CHAPTER 4** ........ 27

**RESULTS AND DISCUSSION** ........ 27

**4.1 ANOVA and Selection of Models** ........ 27

**4.2 Verification of RSM ANOVA Model** ........ 28

**4.3 Diagnostics Plots and Synergetic Influence of Parameters** ........ 29

**4.4 RSM Plot Analysis** ........ 31

**4.4.1 Bulk Unit Weight (BUW)** ........ 32

**4.4.2 Air Voids** ........ 33
**4.4.3 Marshall Stability** ........ 33
**4.4.4 Marshall Flow** ........ 34
**4.5 Model Graphs of Perturbation** ........ 35
**4.6 Numerical Multi-Objective Optimization and Validation of Modeled Results** .... 38
**4.7 Characterization of GeoPOCF and GeoPOCF modified bitumen** ........ 40
**4.7.1 XRD of GeoPOCF-MB** ........ 40
**4.7.2 FTIR of GeoPOCF-MB** ........ 43
**4.7.3 SEM/EDX of GeoPOCF-MB** ........ 44
**CHAPTER 5** ........ 47
**CONCLUSION** ........ 47
**REFERENCES** ........ 48

# List of Figures

FIGURE 1.1 Various Oil Palm Waste Form and Its Derivative .... 1
FIGURE 1.2 Pavement Layers .... 3
FIGURE 2.1 Preparation of Geopolymer Additives .... 8
FIGURE 2.2 Marshall stability testing device .... 10
FIGURE 2.3 Example of 2D and 3D Models Generated by RSM Software .... 12
FIGURE 2.4 POCF powder XRD pattern .... 14
FIGURE 2.5 XRD diffractogram profiles for plain bitumen and POCF-MB at varying dosages .... 15
FIGURE 2.6 POCF FTIR spectrometer .... 16
FIGURE 2.7 FTIR spectra of the OPC60 and GEO60 specimens .... 16
FIGURE 2.8 XRD diffractograms of the fillers: (a) laboratorial fillers and (b) commercial fillers .... 17
FIGURE 2.9 SEM images and mapping with the identification of the geopolymer binder, natural aggregate and microcracks for Series 4 .... 18
FIGURE 2.10 SEM photos of geopolymer concrete after cured for 28 days (a) limestone aggregate and (b) steel slag aggregate .... 18
FIGURE 3.1 Project Workflow .... 19
FIGURE 4.1 Diagnostic plots for all responses .... 30
FIGURE 4.2 Leverage points of all responses .... 31
FIGURE 4.3 Effect of GeoPOCF and bitumen contents on BUW (a) 2D (b) 3D .... 32
FIGURE 4.4 Effect of GeoPOCF and bitumen contents on air voids (a) 2D (b) 3D. 33
FIGURE 4.5 Effect of GeoPOCF and bitumen contents on Marshall stability (a) 2D (b) 3D .... 34
FIGURE 4.6 Effect of GeoPOCF and bitumen contents on Marshall flow (a) 2D (b) 3D .... 35
FIGURE 4.7 Perturbation plot for BUW .... 36
FIGURE 4.8 Perturbation plot for air voids .... 36
FIGURE 4.9 Perturbation plot for Marshall stability .... 37
FIGURE 4.10 Perturbation plot for Marshall flow .... 37
FIGURE 4.11 Numerical optimization ramp for input parameters and output responses .... 39
FIGURE 4.12 The XRD patterns of unmodified bitumen and GeoPOCF-MB .... 41
FIGURE 4.13 Peaks produced by XRD analysis for unmodified bitumen .... 42
FIGURE 4.14 Peaks produced by XRD analysis for unmodified bitumen .... 42
FIGURE 4.15 FTIR spectra of GeoPOCF .... 43
FIGURE 4.16 Combined FTIR spectra of GeoPOCF powder, unmodified bitumen and GeoPOCF-MB .... 44
FIGURE 4.17 SEM images and EDX of unmodified bitumen .... 46
FIGURE 4.18 SEM images and EDX of GeoPOCF-MB .... 46

# List of Tables

TABLE 2.1 POCF chemical compositions ........................................................ 13
TABLE 3.1 Independent experimental variables and their coded levels for the RSM design ........................................................................................................ 25
TABLE 3.2 Experimental design matrix design and their responses ........................ 25
TABLE 4.1 ANOVA for the analysis of responses .................................................. 27
TABLE 4.2 Model verification summary for all responses ...................................... 29
TABLE 4.3 Selected numerical conditions for optimization for Marshall mix design requirements ........................................................................................... 38
TABLE 4.4 Model validation for laboratory and predicted outputs .......................... 39
Table 4.5 GeoPOCF-MB XRD results ...................................................................... 42
TABLE 4.6 Unmodified bitumen XRD results .......................................................... 42
TABLE 4.7 Quantity analysis from EDX on unmodified bitumen and GeoPOCF-MB ...................................................................................................................... 45

# CHAPTER 1

## INTRODUCTION

The introduction part covers on the background of study, problem statement, objectives and study scopes including relevancy and feasibility. In order to have clear understanding of the project work, the background of study will be area of palm oil industry, industrial by-products as geopolymer, and road construction. The problem of this area will be discussed and later providing the solution of the given problem. The objectives and scope of study must be precisely determined prior project execution in order to lead onto project success within the time frame.

### 1.1 Background of Study

Palm oil is one of Malaysia's main industries, contributing for the majority of the country's agricultural industry. Palm oil is the most widely used edible oil in the world, and it is utilized in a variety of consumer items as well as biofuels. After Indonesia, Malaysia is the second-largest producer of palm oil in the world. These two countries together account for more than 80% of worldwide palm oil output. Despite of being most palm oil production, Dungani et al. [1] stated that only 10% of palm oil processing activities provided palm oil and palm kernel oil, with the remaining 90% remaining as biomass or waste until this day. The various oil palm waste form and its derivative [1] can be referred in Figure 1.1.

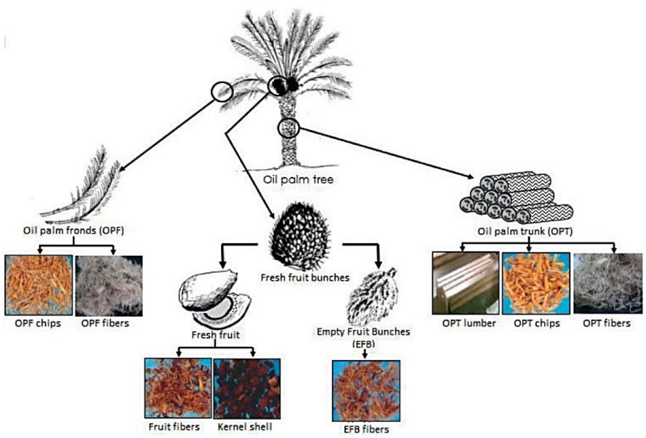


FIGURE 1.1 Various Oil Palm Waste Form and Its Derivative

Apart from the palm oil industry, there are various industries like power generation industry, iron making industry, steel making industry, mining industry and many more released large amount of industrial wastes. These wastes like fly ash, bottom ash, blast furnace slag, metakaolin, and others pose various difficulties in their disposal. Mabroum et al. [2] found out mine waste rocks, tailings, slags, ashes, and sludges are the most common solid wastes or by-products produced during ore mining and enrichment processes. Some of these wastes with geopolymeric binders derived from these industrial by-products can be utilized for some other application.

Malaysia features one of the world's finest road networks, extending over 60,000 kilometers and connecting all of the country's states. Roads in Malaysia are classified into two broad categories, namely federal roads and state roads. Road pavements will not last forever once constructed. For example, flexible pavement typically has a design life of ten years. The road surface will show signs of wear, such as cracking, rutting, and polishing. Maintenance is frequently necessary, and it costs a lot of money. The study on adding additional materials from industrial wastes into roads construction is increasing recently to produce high road performance.

The layer of road consists of sub-base, road base, binder course and wearing course as in Figure 1.2. The asphalt mixtures are used as binder and wearing course. Three main road paving materials are aggregates, asphalt binders, and fillers to produce asphalt mixture. The preparation of the asphalt mixture in Malaysia usually uses Marshall mix design method with meeting the Jabatan Kerja Raya (JKR) Malaysia specifications for pavement design which requires to conduct Marshall stability and flow test. The study from researchers showed that there are many waste materials can be used in road construction industry and it increases pavement performance. Therefore, this research is to conduct study on utilization of industrial wastes into preparation of asphalt mixtures.


FIGURE 1.2 Pavement Layers

Based on past study, it was discovered that there are few publications on bitumen modification using palm oil clinker fines (POCF), encouraging inquiry into the necessity for more extensive studies to develop another study with addition of geopolymer into POCF. Furthermore, modelling and optimizing the synergetic impact of diverse elements affecting the engineering characteristics of bitumen would aid in providing a better understanding of the effects of many variables. The present study is to assess the suitability of GeoPOCF as a sustainable bitumen modifier by using Marshall mix design and testing as well as characterization test.

The preparation of the modified bitumen needs optimum values of mixing parameters for temperature, speed and time by using multimix mixer. Yaro et al. [3] stated that the addition of POCF enhances bitumen stiffness, as evidenced by the plots of conventional characteristics and RSM models where the mixing parameters for temperature, speed, and duration were 140 ˚C, 1000 rpm, and 51.9 min, respectively, according to the multi-objective optimization. Consequently, this study uses the same mixing parameters in order to prepare the geopolymer modified bitumen, GeoPOCF-MB in the laboratory.

In this study, the significance and fitness of the chosen regression model for each variable is tested using variance analysis (ANOVA). The responses are determined using the suggested models. F-test is also used to test the proposed models, which are statistically significant as measured by the p-value with a 95% confidence level. To assess the fitted model's data adequacy and variance, a lack of fit analysis (LOF) is used. F-test is also to ensure that the model has appropriate accuracy (A.P), and standard deviation (S.D) is to examine the model and the data sets' variation from their means. The coefficient variance (C.V.) method is to determine the repeatability of the generated model, which is defined as the ratio of the model's standard error to the average observed outcome value below 10.

**1.2 Problem Statement**

The most typical issues in Malaysia are cracking and rutting of the road surface. It is a major concern since Malaysia's highways are extremely beneficial to the country's economic growth. The failure of asphalt mixes in the pavement structure was frequently identified as the source of road problems. One of the most common strategies for researchers to improve pavement performance is to use industrial waste in the preparation process. However, there is still room for improvement in terms of how this waste is used. There are many researchers did study on the use of industrial waste in pavement materials but the application in industry is still very minimal. Despite several studies in recent years, the comprehensive use of industrial solid waste remains a major challenge for developing countries in sustainable development [4]. As a result, valuing a large quantity of waste in the pavement sector is highly beneficial in terms of decreasing environmental impact while also improving pavement performance.

From previous study, there are various research studies about utilizing waste from palm oil industry into pavement mixture such as palm oil clinker (POC) as a substitute to fine aggregate of stone mastic asphalt (SMA) mixtures [5], POCF as a bitumen modifier [3] and many more. However, none has conducted study on GeoPOCF and bitumen content which improvise volumetric and Marshall properties of asphalt mixture. With the existence of geopolymer substances in pavement mixture might probably increase the stiffness properties in order to increase pavement performance.

The proposed solution is to conduct the project study on asphalt mixtures containing GeoPOCF content and optimize the volumetric and Marshall parameters using RSM software. This software is a tool to show synergetic influences of two or more variables in 2D and 3D model. Rafiq et al. [6] stated that RSM was used to design the experiment and understand the impact of independent variables such aggregate binder ratio, fiber length, and basalt fiber concentration on the Marshall performance parameters of modified asphalt mixtures. It can be said that this project is definitely feasible to execute because there is previous research work has done the same method and statistical tool but different input variables and output responses.

After knowing the optimized parameters, the characterization of the unmodified bitumen, GeoPOCF-MB and GeoPOCF are assessed to identify the molecular interaction and surface morphology on bitumen due to the modification. The samples physical and chemical characteristics are examined by using XRD, FTIR and SEM/EDX analysis. The reason for this analysis is to have better understanding on bitumen modification by comparing three different samples in term of physical and chemical properties.

### 1.3 Objectives of Study

- To optimize the GeoPOCF and bitumen content and develop models on the effect of GeoPOCF modified bitumen on asphalt mixtures volumetric and Marshall parameters by using RSM software.
- To characterize the GeoPOCF and GeoPOCF modified bitumen at optimized content.

### 1.4 Scope of Study

The scope of study will be sequencing into seven main components in order to achieve the project objective above. The first part is to do literature review regarding the project topic. This section is to review some of previous study on the related topic done by the researchers and then find the gap from the past research studies. This component is crucial in initial phase in order to grasp the knowledge on the research area. The second component is to obtain the data for the project work. The laboratory data is used for this project will be input variable which are GeoPOCF and bitumen content and output responses such as bulk unit weight, air voids, Marshall stability and Marshall flow. The laboratory work consists of modified bitumen mixing and Marshall mix design experiment. From the generated experimental RSM design, 13 experimental runs of GeoPOCF-MB blends need to be prepared for preparing the asphalt mixtures and then conducting air voids, BUW, Marshall stability and flow tests. The third component will be working on the RSM software, inserting the response data from 13 experiments with varying content of bitumen and GeoPOCF. Then, the most important component to be conducted is to develop 2D and 3D models for GeoPOCF asphalt mixtures in terms of volumetric and Marshall properties using

RSM software. From here, the optimized data can be developed from the models analysis. Another thing is to conduct analysis on characterization of GeoPOCF powder, unmodified bitumen and GeoPOCF-MB using XRD, FTIR and SEM/EDX analysis. Moreover, next component involves further discussion regarding the findings. The last component is to document all the project work and complete the report.

# CHAPTER 2

## LITERATURE REVIEW AND THEORIES

The literature review section is about literature elements that are relevant to the project. The topics covered for the project can be in multiple topics: (1) geopolymer palm oil clinker fines (GeoPOCF), (2) volumetric parameters and Marshall properties (3) Marshall mix design, (4) utilization of response surface methodology (RSM) and (5) characterization using XRD, FTIR and SEM/EDX analysis.

### 2.1 Geopolymer Palm Oil Clinker Fines (GeoPOCF)

The palm oil industry is expected to grow at a rate of 5% per year, resulting in a huge amount of waste being deposited in landfills. To reduce the environmental impact of these wastes, these can be utilized to replace traditional aggregates in the construction of highway pavements [5]. Based on the previous work on the palm oil clinker fines, the study that has been conducted by the researchers is about to see if utilizing POCF as a bitumen modifier to improve conventional properties is feasible. The action resulted in a stiffer bitumen blend, which results in less penetration and a higher softening point. Thus, it improves the conventional properties of the asphalt bitumen [3].

However, none has conducted the study on adding geopolymer into POCF that might probably increase the conventional properties of asphalt binder. In concrete production, research findings show that geopolymers can achieve comparable or greater shear strength and durability to traditional binders or concrete while leaving a smaller environmental imprint [7]. It can be said that the study on GeoPOCF could be resulted in more resistant to low temperature cracking and rutting deformation compared to previous work which only utilizing the POCF in preparing asphalt bitumen for the pavement. Thus, the possibility of utilizing GeoPOCF as a supplemental asphalt binder modifier is examined in this study to ensure its long-term sustainability.

Hamid et al. [8] revealed on how prepare geopolymers Fly ash and an alkali activator were used to make geopolymer. The alkali activator was a mixture of sodium silicate solution ($Na_2SiO_3$) and sodium hydroxide (NaOH) pallet diluted in water to make an 8-mole (8M) NaOH solution. To activate the alumino-silicate precursors in fly ash, a solution of sodium silicate and sodium hydroxide was used. Similarly, this project uses the same methods and chemical solutions to prepare the geopolymer based, the fly ash will be changed into POCF to produce GeoPOCF. The detailed procedures to produce fly-ash based geopolymer can be seen in Figure 2.1 [8]. The alkaline solution was prepared using sodium hydroxide (8M) and sodium silicate solution with percentages of 100 : 50% by mass respectively, 200 grams of fly ash powder was mixed with 80 grams of the alkaline medium for 6 minutes, the formed slurry was transferred to silicon molds and geopolymers were cured at room temperature (23–25˚C) and in the oven (40˚C) [8].

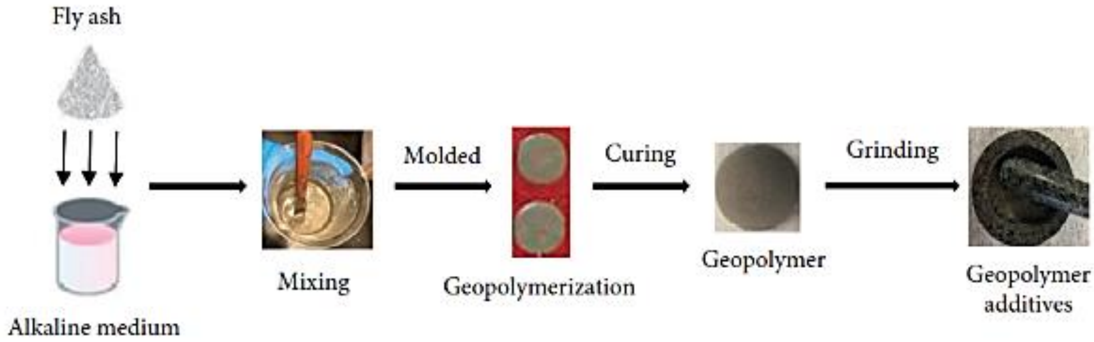


FIGURE 2.1 Preparation of Geopolymer Additives

**2.2 Volumetric Parameters and Marshall Properties**

The Marshall stability and flow test is used to estimate how well the Marshall mix design technique will perform. It can estimate how well an asphalt mixture will perform and the maximum load it can support using the Marshall stability test. Furthermore, the bulk unit weight (BUW) determines the volume of aggregate, bitumen, and GeoPOCF in asphalt mixtures, including solid aggregate particles and voids between them. Besides, the amount of air voids in bituminous materials is an important control criterion for the quality of bitumen that is deposited and compacted. If the air void content is too high, air and water might access. The use of mineral fillers in asphalt was recognized in the early 1900s to enhance the stiffness of the asphalt mixture. Fillers in asphalt mixes increase mixture compatibility, workability, and aggregate-bitumen adhesion bonding while also increasing durability and water resistance [9]. This modification of asphalt mixtures designed to enhance stiffness at high temperatures while maintaining flexibility at lower temperatures. It also improves the visco-elastic properties of bitumen [3]. As shown in previous studies, asphalt penetration values and softening points are critical features in providing stiffness for improved design and optimization of the modified asphalt modification process. Besides from dosage, physical and chemical properties, shape and texture, size and gradation are all important for an asphalt mixture's optimal performance [9]. Therefore, the asphalt binder conventional properties like asphalt penetration values and softening points are the physical and chemical parameters to study in producing stiffness asphalt binder.

For this project volumetric and Marshall properties are taken into account. Marshall Stability is conventional destructive methods are used to calculate the stability of asphalt concrete. Destructive testing is a common practice that is both costly and time-consuming [10]. On the other hand, the air void content (AV), apparent film thickness (AFT), voids in mineral aggregate (VMA), and voids filled with asphalt (VFA) are all common volumetric parameters where these parameters' requirements have been empirically established based on a large amount of laboratory and field data [11] . Both Marshall and volumetric parameters are properties measured of the asphalt mixtures. These properties as well as GeoPOCF and bitumen content are used in this project. Understanding on how these elements interact and impact the modification process is essential and crucial [12].

## 2.3 Marshall Mix Design

The process to get the set responses (air voids, bulk unit weight, Marshall stability and flow) for this project is to prepare the samples by using Marshall mix design. Following ASTM D6927, the Marshall mix design was used and evaluated for compacted samples [13]. The volumetric criteria for determining optimal binder content (OBC) for the control mix were bulk unit weight, total mix voids, mineral aggregate voids, and bitumen filled voids. To maintain the asphalt mixtures' acceptable durability over their service life, each volumetric parameter must be within the range stipulated by JKR, Malaysia. Temperature and traffic loads were included in Marshall mix design to analyze the essential technical parameters for empirical assessment of asphalt mixtures. The volumetric parameters were verified at OBC to confirm that the acquired values were within the prescribed range of AC 14 wearing course in accordance with JKR requirements [14].

From previous work, to develop the Reclaimed Asphalt Pavement (RAP) containing Stone Mastic Asphalt (SMA) mixture in compliance with the ASTM D6926 standard, the standard Marshall mix design was used. RAP and virgin aggregates are combined graded at first, and both RAP and virgin aggregates are baked in an oven to 175–190˚C. Sisal fiber and Waste Engine Oil (WEO) were added to the mixture and well mixed. WEO and other rejuvenators were used to lubricate both RAP and fresh aggregates, as well as soften the aged binder. The needed proportion of bitumen was then added to the SMA mixture, which was then transferred to the Marshall mould, which has a diameter of 101.6 mm and a height of 63.5 ± 1 mm, and examples were compressed by providing 50 blows on each sides [15].

The Marshall stability test as in Figure 2.2 is a standard process for pavement work that is widely used. The Marshall Stability Test is used to establish the stability of bituminous mixtures according to Ministry of Road Transport and Highways (MORTH) requirements, as well as the ideal bitumen concentration for pavements. The Marshall stability test is an empirical test in which no deviations from the usual technique, such as reheating the mixture before preparing the specimens or running the test on the field compacted value, are acceptable [16].


FIGURE 2.2 Marshall stability testing device

## 2.4 Response Surface Methodology (RSM)

Response surface methodology (RSM) is a type of effective method for optimizing process conditions, and it can determine the influence of various factors and their interactions on the indexes under investigation (response value) during experimental study. It can also be used to fit a complete quadratic polynomial model through a central composite experiment, and it can present better experiment design and result expression. In order to access the best performance parameter in this study, the statistical tool RSM was utilized to effectively develop, evaluate, optimize, and finally validate experimentally based findings [6].

Based on previous work, 30 experimental runs of POCF-MB blends were produced and characterized for penetration, softening, and PI tests using the experimental RSM design. The response was subjected to ANOVA in order to create statistical and diagnostic models [3]. It indicates that this statistical analysis and analytical tool coped the problem which is high number of trials needed leads to high cost. The tool assists in boosting process yield without raising costs [17]. Despite the fact that such procedures have no physical basis, they may be effective in reducing the amount of laboratory tests required by the Marshall Mix design, which is heavily tested in many asphalt labs [10].

The influence of GeoPOCF and bitumen content on the Marshall and volumetric properties which are bulk specific density, air voids, Marshall stability and Marshall flow of the geopolymer modified asphalt mixtures can be illustrated in the 2D and 3D surface plots. As example from previous study, the results generated by the RSM software can be referred in Figure 2.3. This example shows the effects of mixing time and POCF content on penetration test [3]. The oval contour shape in the diagnostic plots of 2D and 3D demonstrates sufficient connectivity between the independent variables. From there, it can be said that the content of the POCF dose has a greater impact on penetration than the mixing speed. Therefore, the study of geopolymer modified asphalt mixtures can be optimized and analyzed using RSM software.

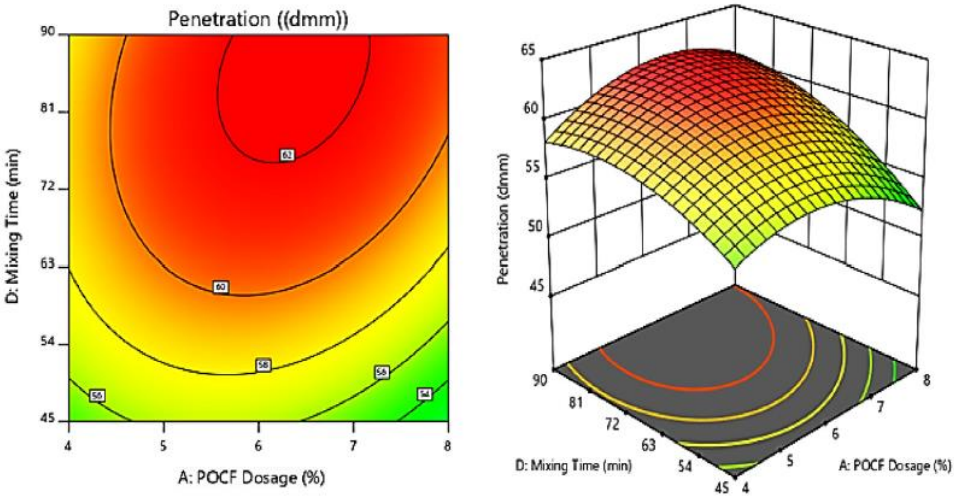


FIGURE 2.3 Example of 2D and 3D Models Generated by RSM Software

## 2.5 XRD, FTIR and SEM/EDX Analysis

The characterization of the samples is to check the physical and chemical properties of the samples on how the modification affects the bitumen characteristics. The characterization will be assessed on GeoPOCF powder, unmodified bitumen and GeoPOCF-MB. The literature review on this analysis will be mainly focusing on previous POCF and POCF modified bitumen papers. POCF chemical compositions are shown in Table 2.1. The table shows that POCF is mostly composed of silica, which accounts for more than half of its composition. Other minor chemicals found in the POCF are aluminum oxide, potassium oxide, calcium oxide, and iron oxide. The POCF could be classified as a class C pozzolanic material based on the collected data since the total of $SiO_2$, $Al_2O_3$, and $Fe_2O_3$ is greater than the minimum criterion of 50%. POCF's pozzolanic behavior is further defined by the presence of high silica and the pozzolanic activity of the amorphous silica. The amorphous silica's reactivity is owing to its thermodynamically unstable silica networks [3].

TABLE 2.1 POCF chemical compositions

| Oxides | Abundance (%) |
|---|---|
| $SiO_2$ | 51.61 |
| $Fe_2O_3$ | 3.87 |
| CaO | 14.50 |
| $Al_2O_3$ | 13.26 |
| $K_2O$ | 5.50 |
| MgO | 1.41 |
| $P_2O_3$ | 4.16 |
| $SO_3$ | 0.85 |

Meanwhile, geopolymers are three-dimensional amorphous to semi-crystalline aluminosilicate materials made from natural or synthetic aluminosilicate minerals, as well as industrial aluminosilicate by-products like fly ash, red mud, slag, metakaolin, perlite, glass, rice husk ash, clay, or a combination of these materials mixed with an alkaline (potassium or sodium hydroxide, potassium/sodium silicate). Geopolymer is an example of an inorganic polymer. The polymerization process requires a rapid reaction of silica (Si) and alumina (Al) in an alkaline environment, resulting in a three-dimensional polymeric chain of Si-O-Al-O bonds [18]. Unlike ordinary Portland cement (OPC) or pozzolanic cements, geopolymer produces compressive strength by polycondensation process of silica, alumina, and a high alkali component [19].

Figure 2.4 displays the X-ray diffraction pattern of POCF [20]. The XRD spectrum of the POCF revealed a quartz-dominated crystallization. The POCF phase is predominantly crystalline, with traces of amorphosity halo of silica oxide and potassium alumina silicate, as shown between 20˚ and 35˚. The materials' mineralogical phases are comparable to those seen in palm oil ash and other agro-waste ash. The waste can only be used as an additive and cannot be used in pozzolanic processes. The pozzolan characteristics of the POCF are the subject of this study since they might be used to change the bitumen.

Furthermore, the existence of substantial peaks in the XRD pattern that correlates to the Joint Committee on Powder Diffraction Standards (JCPDS) suggests that the $SiO_2$ structure is important as the major element in POCF [20]. The predominant phase was discovered to be a-quartz, with the highest peaks being (α-$SiO_2$). Furthermore, the POCF's reference number is 01–075-8320, with peaks corresponding to 20.82˚, 26.62˚, and 39.43˚, and comparisons were done with JCPDS entry card number 00–46-1045 for silicon dioxide/quartz) [21]. It can be concluded that the major components are a-quartz ($SiO_2$), iron oxide ($Fe_2O_3$), and cristobalite ($SiO_2$). The minor phases include grossular [$Ca_3Al_2(SiO_4)_2(OH)_4$] and potassium aluminum phosphate [$K_3Al_2(PO_4)_3$].

Semi-crystalline has a peak at an angle of roughly 21.8˚. The peak diffraction was shifted due to substantial molecular silica-bitumen interactions. In other words, crystallization does not separate the asphaltene molecules from the silica and bitumen. The modified bitumen peaks that fall between the carbon and silica peak zones cause intercalation and peeling, as shown by these data. The results are consistent with earlier research [22] in which bitumen was treated with a silicious substance [21].

As shown in Figure 2.5, XRD was conducted to investigate the characteristic features of ordinary bitumen and POCF-MB [21]. The basic bitumen was found to be completely amorphous (non-crystalline), with no discernible peaks. The integration of POCF, on the other hand, altered the base bitumen from amorphous to semi-crystalline, indicating the influence of POCF modification on the structural characteristics of the base bitumen.

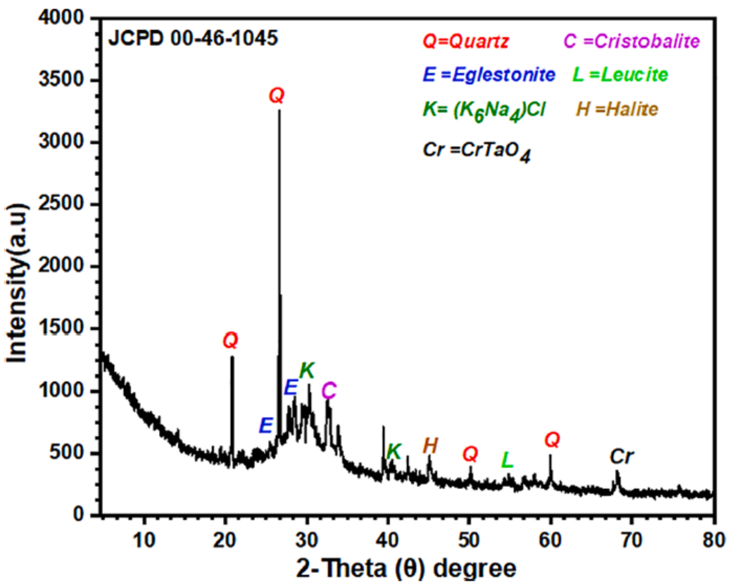


FIGURE 2.4 POCF powder XRD pattern

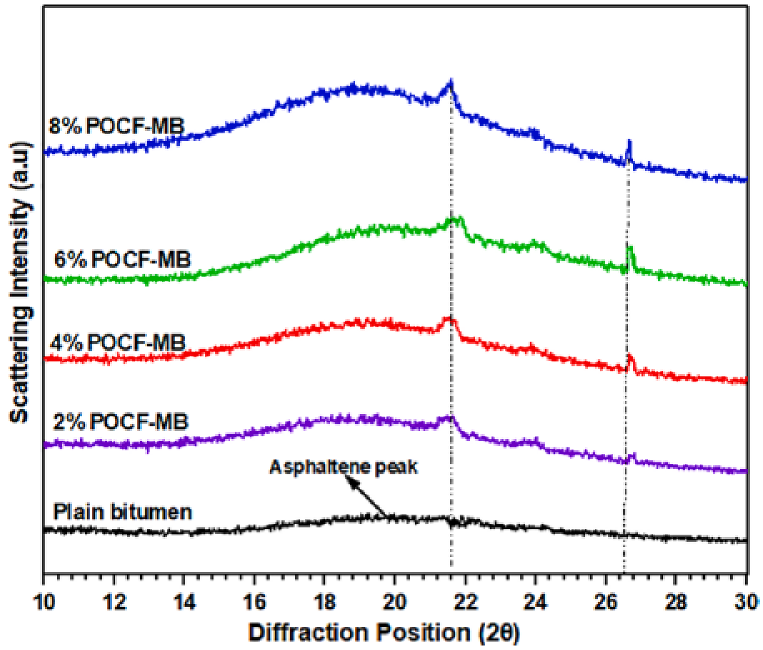


FIGURE 2.5 XRD diffractogram profiles for plain bitumen and POCF-MB at varying dosages

The POCF FTIR analysis findings are shown in Figure 2.6 [21]. The quartz and cristobalite minerals in POCF are also identified using FTIR measurements. Organic carbon has a peak at around 3000 $cm^{-1}$ in FTIR spectra. The mineral quartz is one of the most significant in POCF, and it is usually present. The occurrence of two bands at 997 and 1033 $cm^{-1}$, induced by vibrations in the stretching and bending bands of (Si-O) in $SiO_4$, indicates the presence of crystalline phases such as quartz minerals in the samples. Peaks ranging from 480 to 554 $cm^{-1}$ were caused by Si-O-Si vibration bending. In addition, the vibrations of O-H stretching and H-O-H bending are represented by 3233 and 3443 $cm^{-1}$ [21].

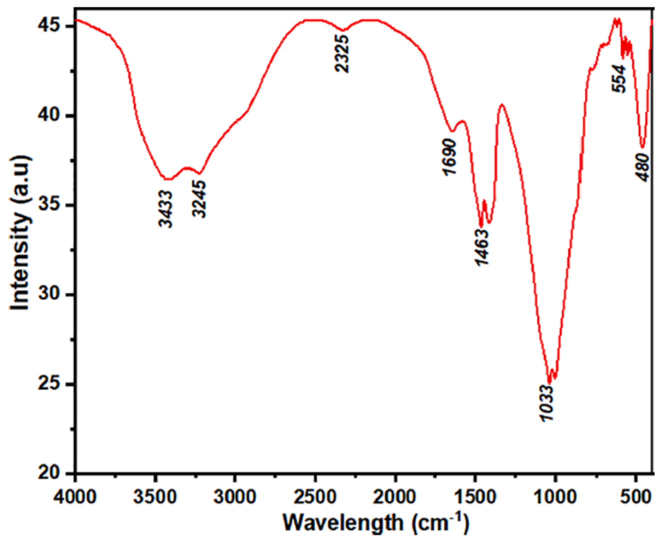


FIGURE 2.6 POCF FTIR spectrometer

There was study on FTIR analysis was conducted to characterize the specimens and indicate the pattern of chemical reaction changes. The concrete mix proportions for casting of the specimens with the standard strength grades of 60 MPa for the ordinary Portland cement (OPC)-based concrete (OPC60) and geopolymer concrete (GEO60). FTIR spectra of the specimens was analyzed after the exposure to fire at 500 and 1200 ˚C are shown in Figure 2.7 [23]. The 1000 $cm^{-1}$ band indicates that formation of geopolymers was taking place, where the transition of $SiO_2$ and $Al_2O_3$ occurred due to the chemical reaction between fly ash and an alkaline solution [24].

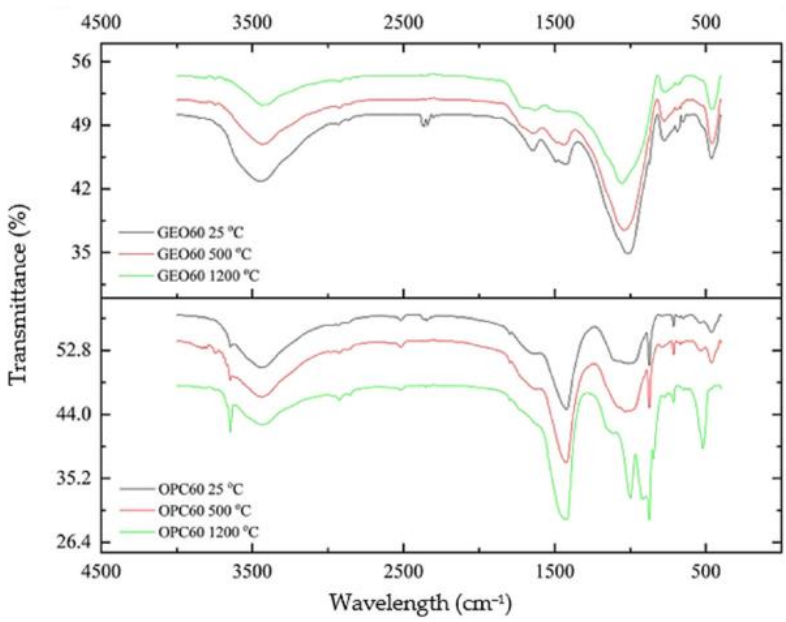


FIGURE 2.7 FTIR spectra of the OPC60 and GEO60 specimens

Image analysis (SEM), laser particle size analysis, XRF (X-ray fluorescence), and XRD (X-Ray diffraction) were used to determine the surface micromorphology, particle size distribution, chemical composition, and physical phase, respectively. This can help describe the qualities of fillers and guarantee that variables other than morphological parameters aren't affecting the active adhesion performance of mastics with various fillers [23].

Figure 2.8 shows the XRD diffraction pattern of the fillers [23]. The XRD diagrams of Ball grinding mill-Filler (BF), Mortar grinder–Filler (MF), and Hammer-Filler (HF) are shown in Figure 2.8 (a). Because just a physical approach is employed to modify the morphologies of filler, three distinct types of filler with various crush methods have the same composite. Figure 2.8 (b) shows an XRD diagram of commercial filler or and Jaw crusher-Filler (JF). The strongest peak in the diffraction patterns of two types of filler is seen at 29-31, which corresponds to $CaCO_3$ [23].

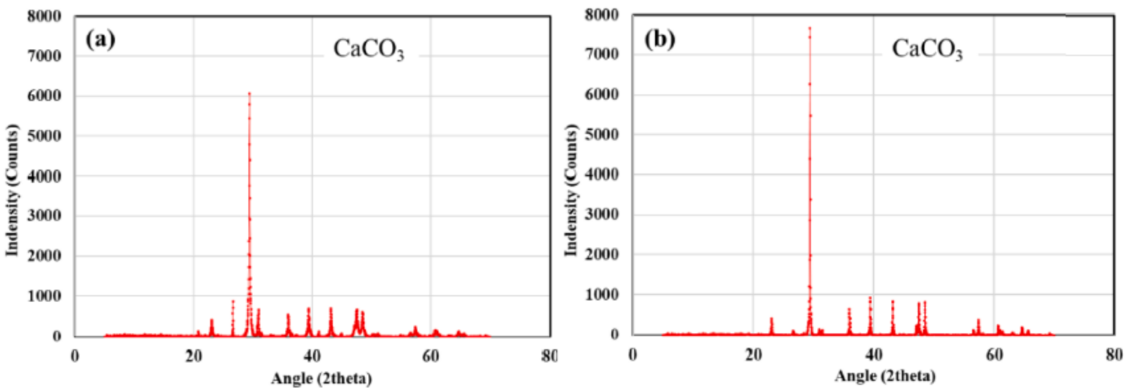


FIGURE 2.8 XRD diffractograms of the fillers: (a) laboratorial fillers and (b) commercial fillers

The study on geopolymer concrete was conducted. At low magnification, Figure 2.9 shows a SEM picture (A) and mapping (B) of Series 4 [19]. Unreacted fly ash was discovered. These unreacted particles lowered the compressive strength of the geopolymer structure. Natural siliceous aggregate (quartz) and some tiny particles of calcite and dolomite were also found due to the composition stated in the mapping as in Figure 2.9 (B). Microcracks were also discovered in the geopolymer binder as in Figure 2.9 (A). These microcracks may have formed as a result of the sample collection (tiny fragments) or polishing procedure [19].

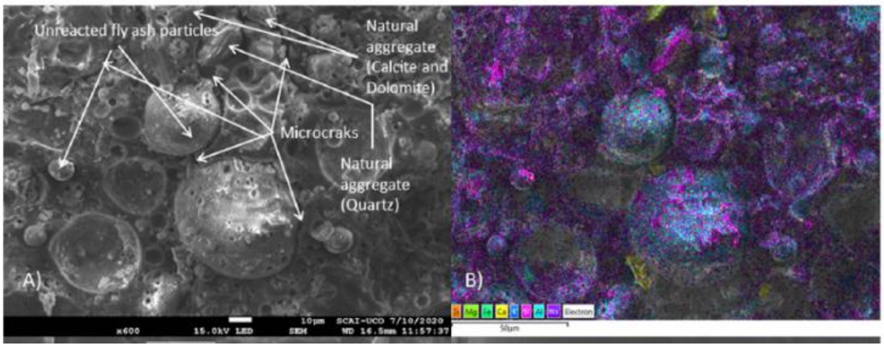


FIGURE 2.9 SEM images and mapping with the identification of the geopolymer binder, natural aggregate and microcracks for Series 4

The SEM images and EDS mapping scan at the geopolymer concrete's interfacial transition zone (ITZ) are shown in Figure 2.10 [25]. Between the limestone aggregate and metakaolin-based geopolymer paste, a distinct aggregate/gel interface and an apparent micro-crack can be seen in Fig. 2.10 (a). The shift was less visible in the metakaolin-based geopolymer produced with basic oxygen furnace steel slag aggregate (BOF SSA) as in Figure 2.10 (b). Micro-cracks caused by stress concentration might easily cause concrete to fracture. For metakaolin-based geopolymer produced by BOF SSA, the good bonding interface explained a strong aggregate-binder interface yielded stronger compressive strength [25].

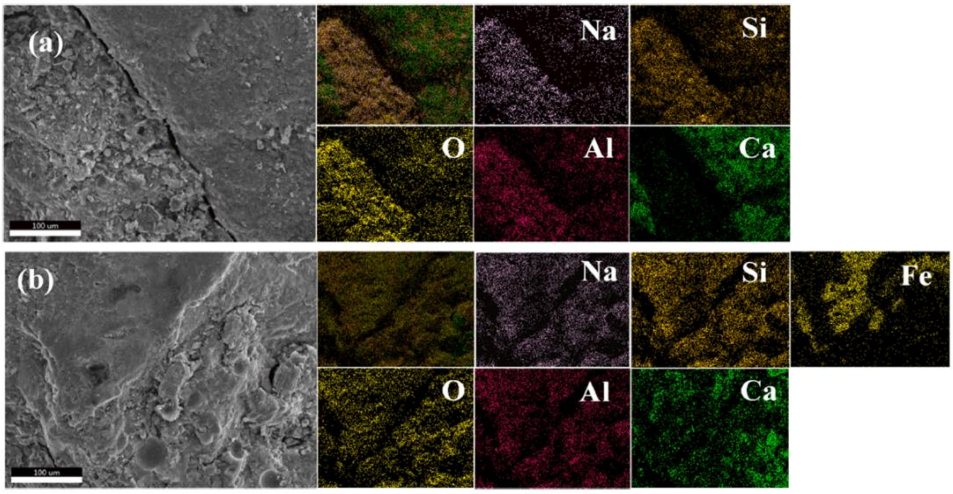


FIGURE 2.10 SEM photos of geopolymer concrete after cured for 28 days (a) limestone aggregate and (b) steel slag aggregate

# CHAPTER 3

## METHODOLOGY

In order to achieve the project objectives, the project workflow and Gantt chart are prepared prior the project execution. In this chapter, the project workflow will be explained briefly with the aid of flow diagram as shown in Figure 3.1.

### 3.1 Project Workflow

The project workflow below in Figure 3.1 is the feasible way to do optimization of the volumetric and Marshall properties of asphalt mixtures by using RSM software. The task is to generate 2D and 3D models and then generate optimized data on those properties in order to produce the optimum standard parameters for geopolymer modified asphalt mixture for road pavement. Another aim is to characterize GeoPOCF and GeoPOCF-MB in terms of physical and chemical characteristics.

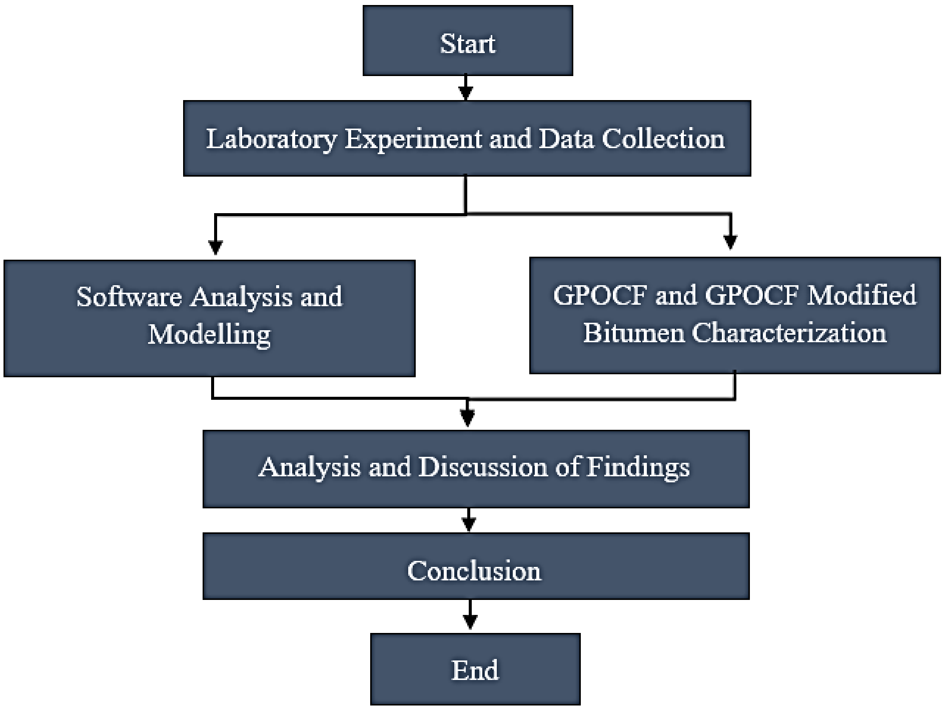


FIGURE 3.1 Project Workflow

### 3.1.1 Laboratory Experiment and Data Collection

For the data collection, this study uses the primary data which is from laboratory data. The laboratory works is using Marshall method by preparing the specimens and then conducting tests to obtain Marshall and volumetric properties which are bulk unit weight, air voids, Marshall stability and Marshall flow by using Marshall testing apparatus. From the generated experimental RSM design, 13 experimental runs of GeoPOCF-MB blends need to be prepared producing the asphalt mixtures and then conducting air voids, BUW, Marshall stability and flow tests. The preparation of asphalt mixtures using GeoPOCF, bitumen and aggregates can be referred in procedure (a) while the testing on asphalt mixtures can be referred in procedure (b).

**(a) Preparation of asphalt mixtures**

| Procedures | Pictures |
|---|---|
| 1. Mixing of GeoPOCF and bitumen content at temperature, speed, and duration were 140˚C, 1000rpm, and 51.9mins, respectively. |  |
| 2. The aggregate was heated in the oven at 150°C for 2 hours. |  |
| 3. An appropriate amount of GeoPOCF-MB was added into the aggregate using weight scale to get overall weight of 1100g. |  |

| | |
|---|---|
| 4. The mixing process was done under heated condition using stove. |  |
| 5. The asphalt mixture was poured into steel beaker to be compacted. The mix were compacted in a 100mm diameter steel mould which were also kept at 150°C. |  |
| 6. The asphalt mixture inside the mould was evenly distributed by tamping with a steel rod. |  |
| 7. The asphalt mixture was placed in the Marshall Compacter to make the sample more compact by applying 75 blows on each side. |  |
| 8. After the temperature of the mould has reached room temperature, the asphalt mixture was extruded from the steel mould using an extruder and left for one day to perform Marshall testing. |  |
| 9. Step 1-8 were repeated until another 12 asphalt mixtures were obtained. (13 samples in total) | |

**(b) Testing on asphalt concrete**

| Procedures | Pictures |
|---|---|
| 1. The mass of asphalt mixture was weighted and recorded. |  |
| 2. The asphalt mixture was placed in the buoyancy balance. |  |
| 3. The reading on the weight scale was observed and recorded as weight in water. |  |
| 4. The asphalt mixture was dried off and weighted again as dried weight. |  |
| 5. The asphalt mixture was place in a water bath with a temperature of 60°C for 30 minutes. |  |

| | |
|---|---|
| 6. After that, the asphalt mixture was placed in a Marshall stability machine. |  |
| 7. Flow meter was attached in the Marshall stability machine. |  |
| 8. The value of stability and flow were observed on the machine and recorded. |  |
| 9. Step 1-8 were repeated for other 12 asphalt mixtures. (13 samples in total) | |

### 3.1.2 Software Analysis and Modelling

The 13 experimental data collected will be inserted into RSM software to create 2D and 3D models. The data used are input variables which are GeoPOCF and bitumen content and output responses such as bulk unit weight, air voids, Marshall stability and Marshall flow. By using this model will have analysis and optimization of the GeoPOCF and bitumen content in order to achieve high stiffness of geopolymer modified asphalt mixture. RSM is a mathematical and statistical method for creating interactions between different factors in experimental design while optimizing relevant parameter conditions and determining the best possible response. The independent numeric variable in this project is the input variables, while the dependent numeric variable is the output responses. The responses are assessed via a hand-on experiment using RSM input variables, which are then analyzed to find the best fit model that fulfils the correlation between input and output parameters. The proper regression model for optimal assessment for two independent variables in this study is expressed in Eq. (1) [26].

$$Y = \beta_0 + \sum_{k=1}^{n} \beta_i x_i + \sum_{k=1}^{n} \beta_{kk} x_k^2 + \sum_{k=1}^{n} \sum_{l=1}^{n} \beta_{kl} x_k x_l + \varepsilon \tag{1}$$

Where Y is the response (i.e., BUW, air voids, Marshall stability and Marshall flow) and $x_k$ and $x_l$ are the two independent variables (GeoPOCF and bitumen content). Where $\beta_0$ represents the fixed response value of the design center. $\beta_{kk}$ and $\beta_{kl}$ are constant intercept for linear, quadratic, and interaction coefficients, respectively. And the model's random error and the range of independent variables evaluated are referred to as both $\varepsilon$ and n. Because of its ability to diagnose the significant relationship between factors and responses at many levels, the central composite design (CCD) was used to conduct RSM studies [27].

The high and low values were considered to the boundaries of specific variables in this study. Table 3.1 illustrates the actual (uncoded) and coded values for independent design variables. The RSM software generates trial runs after inputting the various levels for each response. In this setting, 13 experimental design matrices were created at random for GeoPOCF and bitumen content. For four responses, namely air voids, BUW, Marshall stability and Marshall flow, the five central point replications were performed to get an accurate estimate of the experimental and error assessment. The entire experimental matrix based on the responses of Marshall testing is shown in Table 3.2.

TABLE 3.1 Independent experimental variables and their coded levels for the RSM design

| Independent variables | Symbol | Coded variables level | | |
|---|---|---|---|---|
| | | Low (-1) | Medium (0) | High (+1) |
| **GeoPOCF content (%)** | A | 0 | 4 | 8 |
| **Bitumen content (%)** | B | 4 | 5 | 6 |

TABLE 3.2 Experimental design matrix design and their responses

| Run | Independent variables | | Response parameters | | | |
|---|---|---|---|---|---|---|
| | GeoPOCF content (%) | Bitumen content (%) | BUW | Air Voids (%) | Stability (N) | Flow (mm) |
| 1 | 0 | 4 | 2.325 | 6.39 | 12.93 | 2.71 |
| 2 | 4 | 5 | 2.394 | 4.23 | 17.09 | 3.69 |
| 3 | 4 | 6 | 2.338 | 3.19 | 14.97 | 4.24 |
| 4 | 4 | 5 | 2.396 | 4.19 | 17.11 | 3.67 |
| 5 | 8 | 5 | 2.377 | 5.32 | 15.67 | 4.31 |
| 6 | 0 | 6 | 2.339 | 3.41 | 14.98 | 3.61 |
| 7 | 0 | 5 | 2.344 | 4.71 | 16.1 | 2.6 |
| 8 | 4 | 4 | 2.388 | 7.26 | 16.54 | 3.01 |
| 9 | 4 | 5 | 2.399 | 4.16 | 17.12 | 3.7 |
| 10 | 8 | 6 | 2.313 | 3.16 | 11.72 | 4.72 |
| 11 | 8 | 4 | 2.392 | 8.37 | 16.64 | 3.61 |
| 12 | 4 | 5 | 2.409 | 4.2 | 17.89 | 3.71 |
| 13 | 4 | 5 | 2.403 | 4.14 | 17.69 | 3.68 |

The validation test is performed after the optimal values of input variables have been obtained in order to validate the RSM software's results. Three asphalt mixtures were prepared using same procedures to get the average response values. The RSM response parameters were then compared to the laboratory data.

### 3.1.3 GeoPOCF and GeoPOCF-MB Characterization

The characterization work on the GeoPOCF powder, GeoPOCF-MB and unmodified bitumen specimens which were prepared prior the XRD, FTIR and SEM/EDX tests. The findings were discussed and evaluated for the documentation after receiving the results on XRD, FTIR and SEM/EDX analysis.

The purpose of the sample characterization was to have better insight on sample characteristic in terms of physical and chemical properties. The XRD analysis for this study was conducted to determine the amount or content of elements or compounds and compare between unmodified bitumen and GeoPOCF-MB. Besides, the FTIR analysis was carried out to explore the functional groups present in the GeoPOCF powder, GeoPOCF-MB and unmodified bitumen used in the present study. Lastly, the SEM/EDX analysis was utilized to analyze the surface morphology of the unmodified bitumen and changes in the surface morphology of the GeoPOCF-MB.

### 3.1.4 Analysis and Discussion of Findings

The obtained results from RSM software modelling and characterization of GeoPOCF powder, GeoPOCF-MB and unmodified bitumen using XRD, FTIR and SEM/EDX analysis were interpreted and discussed in order to ensure the project objectives achieved. The objectives are to characterize the GeoPOCF and GeoPOCF-MB and to optimize the GeoPOCF and bitumen content and develop a model on the effect of GeoPOCF modified bitumen on asphalt mixtures volumetric and Marshall parameters by using RSM software.

# CHAPTER 4

## RESULTS AND DISCUSSION

### 4.1 ANOVA and Selection of Models

Based on Table 4.1, it depicts the ANOVA findings for all responses which are BUW, air voids, Marshall stability and Marshall flow. The analysis shows that the model term is significant for all responses where "Prob > F" is < 0.05 (significant at 95% confidence interval). The quadratic models were generated for BUW, air voids and Marshall stability, while linear model was generated for Marshall flow. The generated models are based on the highest order polynomial where the additional terms are significant, and the model is not aliased. In addition, the selected model should have insignificant lack-of-fit.

TABLE 4.1 ANOVA for the analysis of responses

| Response | SS | DOF | MS | F-value | P-value | Observation | Model performance |
|---|---|---|---|---|---|---|---|
| **BUW** | | | | | | | |
| **Model** | 0.0129 | 5 | 0.0026 | 33.28 | < 0.0001 | significant | Quadratic |
| **Residual** | 0.0005 | 7 | 0.0001 | - | - | - | |
| **Lack of Fit** | 0.0004 | 3 | 0.0001 | 3.75 | 0.1170 | not significant | |
| **Pure Error** | 0.0001 | 4 | 0.0000 | - | - | - | |
| **Cor Total** | 0.0135 | 12 | - | - | - | - | |
| **Air voids** | | | | | | | |
| **Model** | 30.32 | 5 | 6.06 | 109.47 | < 0.0001 | significant | Quadratic |
| **Residual** | 0.3878 | 7 | 0.0554 | - | - | - | |
| **Lack of Fit** | 0.3829 | 3 | 0.1276 | 103.76 | 0.0003 | significant | |
| **Pure Error** | 0.0049 | 4 | 0.0012 | - | - | - | |
| **Cor Total** | 30.71 | 12 | - | - | - | - | |
| **Marshall Stability** | | | | | | | |
| **Model** | 39.83 | 5 | 7.97 | 73.81 | < 0.0001 | significant | Quadratic |
| **Residual** | 0.7554 | 7 | 0.1079 | - | - | - | |
| **Lack of Fit** | 0.1746 | 3 | 0.0582 | 0.4009 | 0.7607 | not significant | |
| **Pure Error** | 0.5808 | 4 | 0.1452 | - | - | - | |
| **Cor Total** | 40.58 | 12 | - | - | - | - | |
| **Marshall Flow** | | | | | | | |
| **Model** | 4.06 | 2 | 2.03 | 73.02 | < 0.0001 | significant | Linear |
| **Residual** | 0.2777 | 10 | 0.0278 | - | - | - | |
| **Lack of Fit** | 0.2767 | 6 | 0.0461 | 184.48 | < 0.0001 | significant | |
| **Pure Error** | 0.0010 | 4 | 0.0003 | - | - | - | |
| **Cor Total** | 4.33 | 12 | - | - | - | - | |

Equations (2)-(5) indicates the model equations computed for all responses. For given values of each element, the equation in terms of real factors can be used to create predictions about the response. For each factor, the levels should be indicated in the original units.

$$BUW = 1.63299 + 0.047422(GeoPOCF) + 0.284601(Bit.Cont.) - 0.005812(GeoPOCF * Bit.Cont.) - 0.001909(GeoPOCF^2) - 0.028052(Bit.Cont.^2) \quad (2)$$

$$Air\ Voids = 29.09779 + 0.553513(GeoPOCF) - 8.40307(Bit.Cont.) - 0.139375(GeoPOCF * Bit.Cont.) + 0.030108(GeoPOCF^2) + 0.691724(Bit.Cont.^2) \quad (3)$$

$$Stability = -32.14549 + 2.97292(GeoPOCF) + 18.18181(Bit.Cont.) - 0.435625(GeoPOCF * Bit.Cont.) - 0.099246(GeoPOCF^2) - 1.71793(Bit.Cont.^2) \quad (4)$$

$$Flow = 0.315385 + 0.155000(GeoPOCF) + 0.540000(Bit.Cont.) \quad (5)$$

## 4.2 Verification of RSM ANOVA Model

Based on Table 4.2, it shows the significance of all responses from the ANOVA analysis using the P-value < 0.05, which corresponds to the 95% confidence interval, the fit statistic, and validation for all responses. Because the difference is smaller than 0.2, the Predicted $R^2$ of all responses is reasonably close to the Adjusted $R^2$. In the meanwhile, adequate precision (AP) is a criterion that assesses the signal-to-noise ratio. It is really desirable to have a ratio of more than 4. The AP values for the BUW, air voids, Marshall stability and flow are 14.8, 34.49, 25.92 and 28.98, showing that the model is adequate, acceptable and can be used to navigate the design region. A good signal is shown by the ratio of all responses. To navigate the design area, it can be chosen any models. Furthermore, the standard deviation (SD) for the coefficient of variance (CV) following analysis was significantly smaller than the obtained mean values for all of the models tested, indicating that the analysis of variances was adequate and suitable. The lower the standard deviation of the created model is compared to its mean, the more variation it has with the test data. As a result, experimental data yielded reduced uncertainty in the model generated. According to the findings, the generated model is desired, acceptable, and appropriate for modelling and optimization of input variables.

TABLE 4.2 Model verification summary for all responses

| Responses | Model P-value | $R^2$ | Adj. $R^2$ | Pred. $R^2$ | AP | F-value | SD | Mean | CV% |
|---|---|---|---|---|---|---|---|---|---|
| **BUW** | < 0.0001 | 0.9596 | 0.9308 | 0.7431 | 14.7998 | 33.28 | 0.0088 | 2.37 | 0.3721 |
| **Air voids (%)** | < 0.0001 | 0.9874 | 0.9784 | 0.9124 | 34.4948 | 109.47 | 0.2354 | 4.83 | 4.88 |
| **Stability (N)** | < 0.0001 | 0.9814 | 0.9681 | 0.9374 | 25.9209 | 73.81 | 0.3285 | 15.88 | 2.07 |
| **Flow (mm)** | < 0.0001 | 0.9359 | 0.9231 | 0.8706 | 28.9796 | 73.02 | 0.1667 | 3.64 | 4.58 |

## 4.3 Diagnostics Plots and Synergetic Influence of Parameters

As illustrated in Figure 4.1, diagnostic plots to fit statistics were developed to evaluate the appropriateness and normal distribution of the data. Plots of predicted and laboratory values were also evaluated to get a better idea of how well the models worked. In addition, almost all points were equitably distributed very close to the equality line in all of the response's diagnostic plots, indicating that the models developed have appropriate fitting precision. Furthermore, the plots show a positive correlation between anticipated and laboratory results since all points inside the straight line were represented [26].

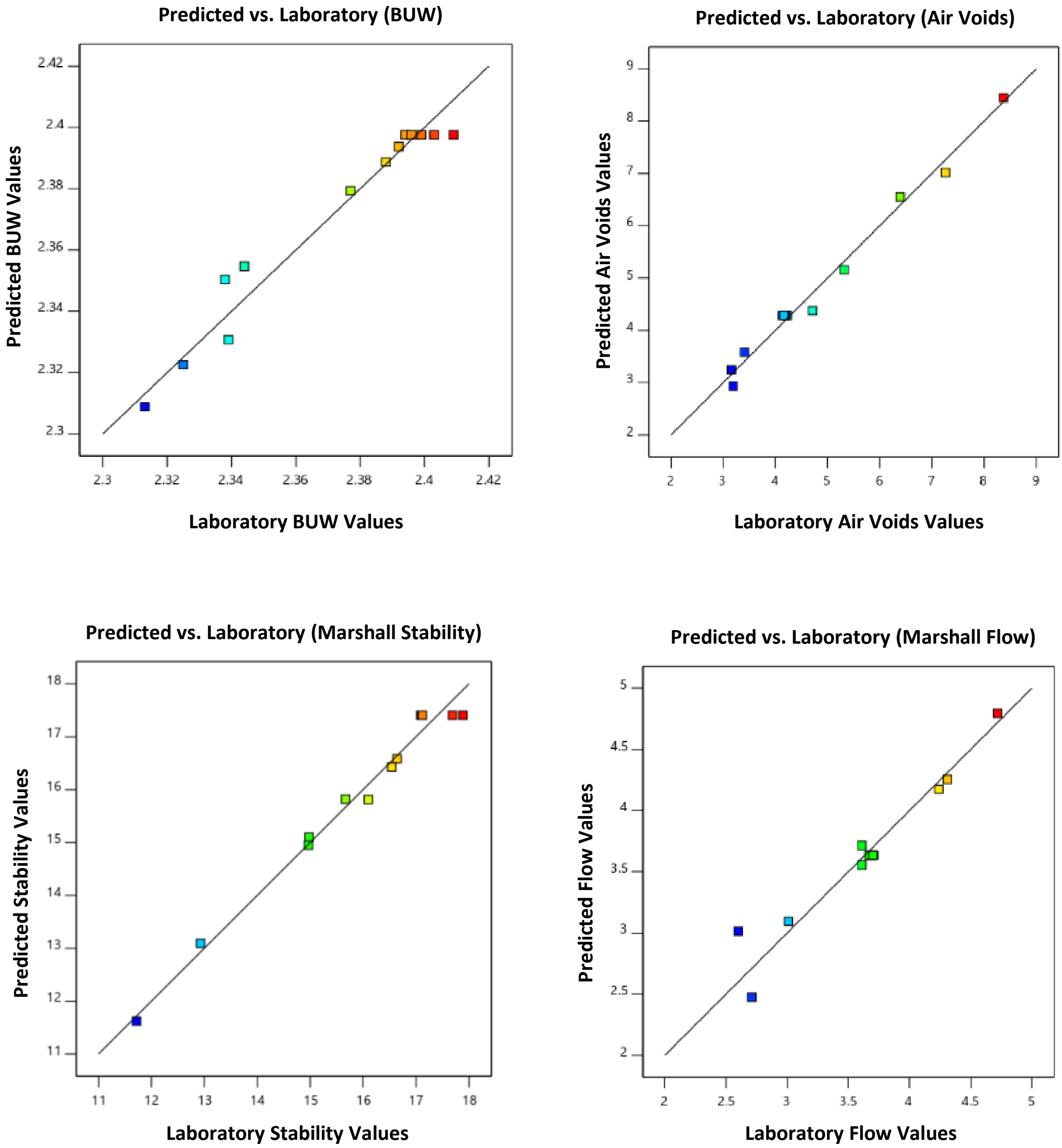


FIGURE 4.1 Diagnostic plots for all responses

The amount each point influences the model fit is measured by leverage. When a point's leverage is 1.0, the model matches the observation perfectly. Figure 4.2 demonstrates that the design points of leverage variation are not close to the value of one, it indicates that all of the points are below one showing that the results are having an impact on the regression models.

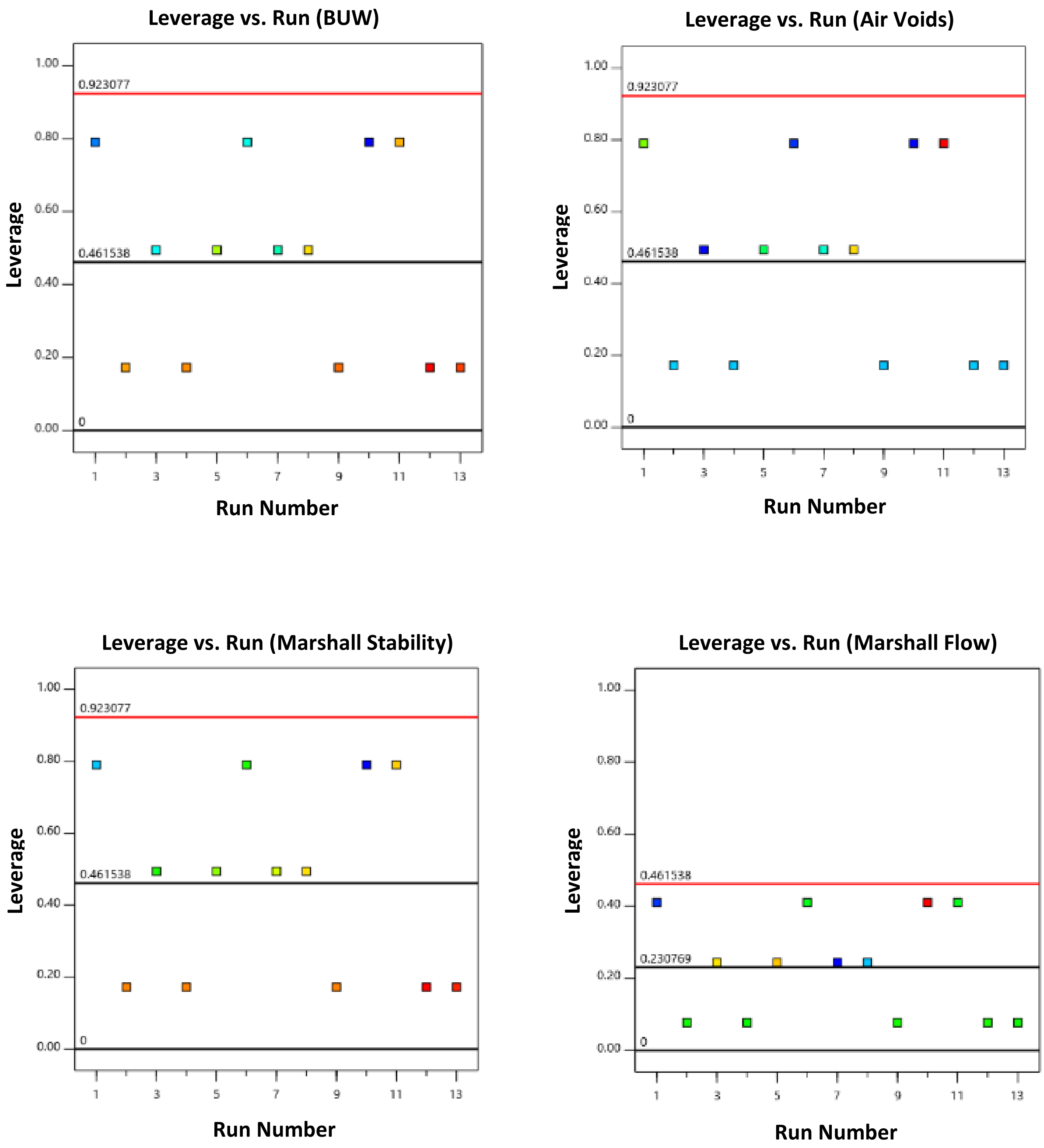


FIGURE 4.2 Leverage points of all responses

### 4.4 RSM Plot Analysis

Surface plots are often useful for examining any potential correlations between variables. The effect of GeoPOCF and bitumen content on BUW, air voids, Marshall stability and flow ware studied and displayed using 2D and 3D contour plots to demonstrate the influence of input variables on BUW, air voids, Marshall stability and flow, as shown in Figures 4.3 until 4.6. The influence of the interaction between the factors and the responses is depicted by the colours in those charts. In all graphs, the blue to red colour indicates a more substantial and significant reaction value. These graphs show how the impact of synergetic interaction among mixing parameter factors might well be significant.

### 4.4.1 Bulk Unit Weight (BUW)

Figure 4.3 shows the interaction effects of the two independent variables, GeoPOCF and bitumen content on the dependent variable, BUW. According to the 2D and 3D diagnostic plots in Figure 4.3, both independent variables have a beneficial impact on the BUW, as the BUW values rise up to roughly 7% of the GeoPOCF content and then remain constant until it reaches 8% of the GeoPOCF. When it comes to bitumen content, there is a little increase in BUW values from 4 to 5.5% bitumen amount, and then a drop between 5.5 and 6% bitumen content. Consequently, greater GeoPOCF quantities and bitumen compositions of 4 to 5.5% result in the greatest BUW values. The rise in BUW values with increasing GeoPOCF content in modified asphalt mixtures might be due to the GeoPOCF at higher contents filling the spaces between the aggregates in compacted modified asphalt mixtures [26].

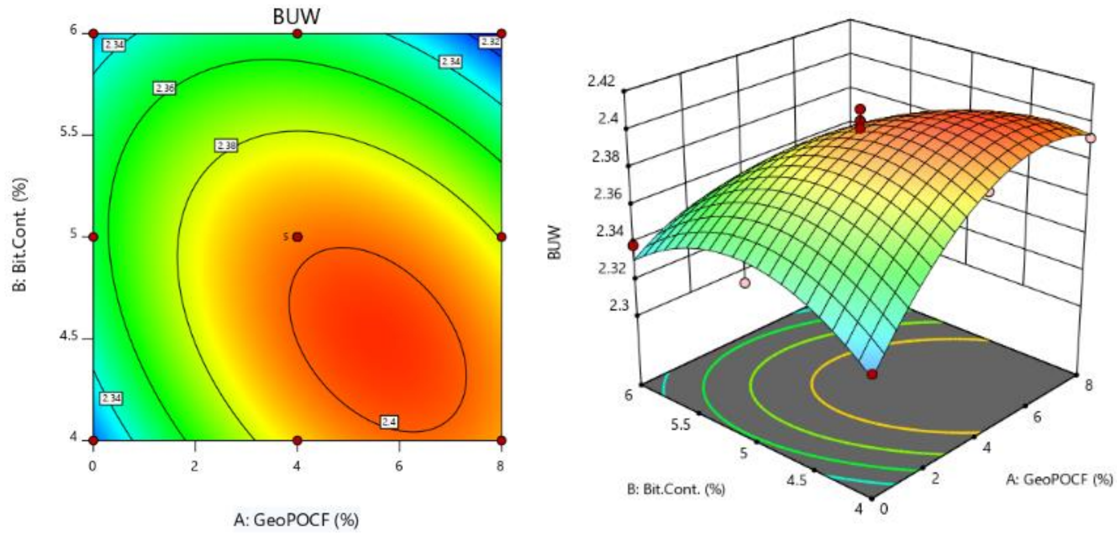


FIGURE 4.3 Effect of GeoPOCF and bitumen contents on BUW (a) 2D (b) 3D

### 4.4.2 Air Voids

The interaction influence of the GeoPOCF and bitumen contents on the air voids is less substantial, since the contour lines are in between oval shapes and linear, according to the 2D contour plot in Figure 4.4. The bitumen amount has a greater influence on the air voids of the GeoPOCF-modified asphalt mixes than the GeoPOCF concentrations, as demonstrated in the 3D plots in Figure 4.4. When GeoPOCF content is added to the mixture, the air voids values initially fell, and lower air voids values were obtained between 2 and 6% GeoPOCF content, after which it increases with increasing the additional GeoPOCF content. This trend was probably caused by the increased GeoPOCF that needed to be coated with bitumen. The air voids decreases when bitumen content increases happened due to the bitumen content filling the voids in the asphalt mixtures.

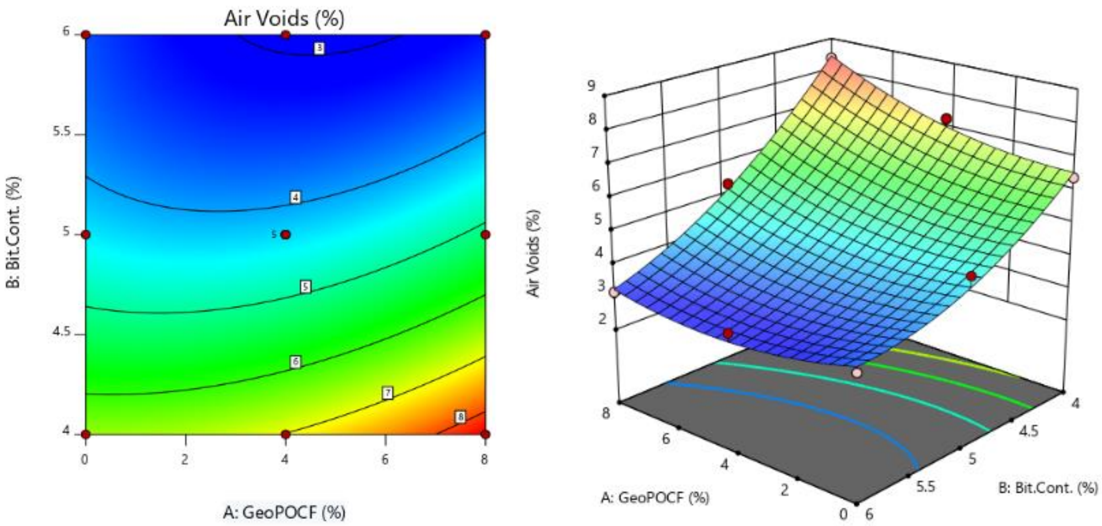


FIGURE 4.4 Effect of GeoPOCF and bitumen contents on air voids (a) 2D (b) 3D

### 4.4.3 Marshall Stability

The relationship between the dependent variable, Marshall stability and the independent variables, GeoPOCF and bitumen content is shown in Figure 4.5. The perfect interaction between the variables is indicated by the elliptical shape and reddish colour of the 2D plots in Figure 4.5 [26]. Both independent factors have a significant impact on the Marshall stability, according to the

Figure 4.5. The Marshall stability values rapidly increase when the GeoPOCF content in the mixtures rises from 0 to 7% and the bitumen percentage rises from 4 to 5.5%. However, when bitumen content exceeds 5.5%, the Marshall stability values decline, and when GeoPOCF content exceeds 7%, the Marshall stability values remain constant. Furthermore, the 2D and 3D graphs in Figure 4.5 reveal that an optimal performance range exists.

The reason that can be probably associated with the rise in Marshall stability is the material inside GeoPOCF, which makes it a useful material for strengthening asphalt mixtures. The GeoPOCF's high tensile strength can also help to improve Marshall stability, allowing the material in reinforced asphalt mixtures to resist breaking, segregation, and balling during mixing and compaction. The Marshall Stability is significantly affected by both the independent variables GeoPOCF and bitumen concentration. The Marshall Stability has been displayed to be more affected by GeoPOCF content than by bitumen concentration.

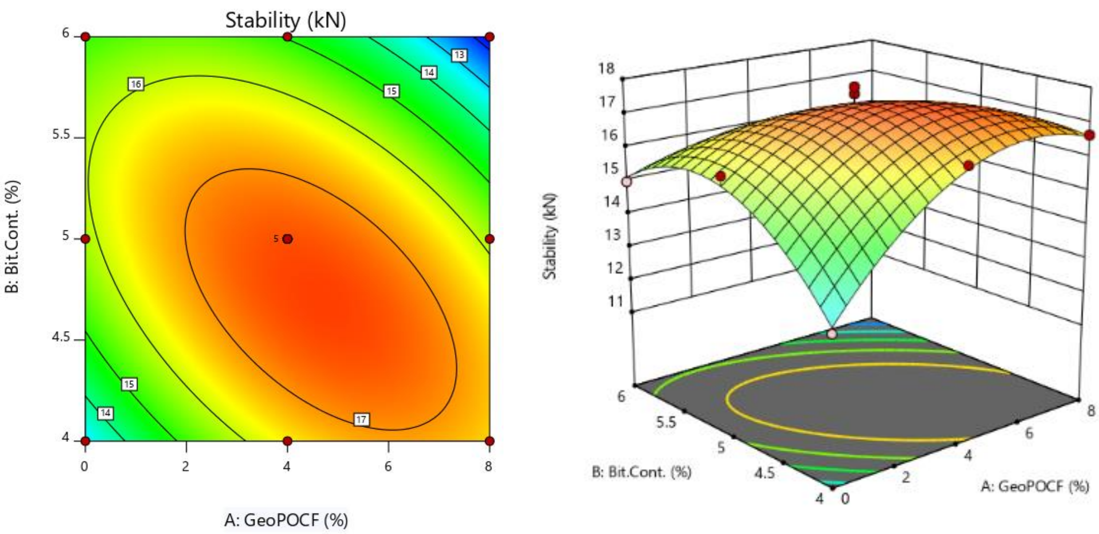


FIGURE 4.5 Effect of GeoPOCF and bitumen contents on Marshall stability (a) 2D (b) 3D

### 4.4.4 Marshall Flow

The amount of deformation generated by the application of load on asphalt mixtures is known as Marshall Flow. The flow value is also used to calculate the reversibility of the asphalt pavement's wearing course under traffic loads [26]. The connection between GeoPOCF and bitumen concentration was found to be linear in this study, as shown in Figure 4.6, and their influence on Marshall flow was identical, as observed in the RSM's 2D contour and 3D surface plot. Because of the linear relationship, increasing any of the variables, GeoPOCF and bitumen contents can result in increased flow values of the modified asphalt mixtures.

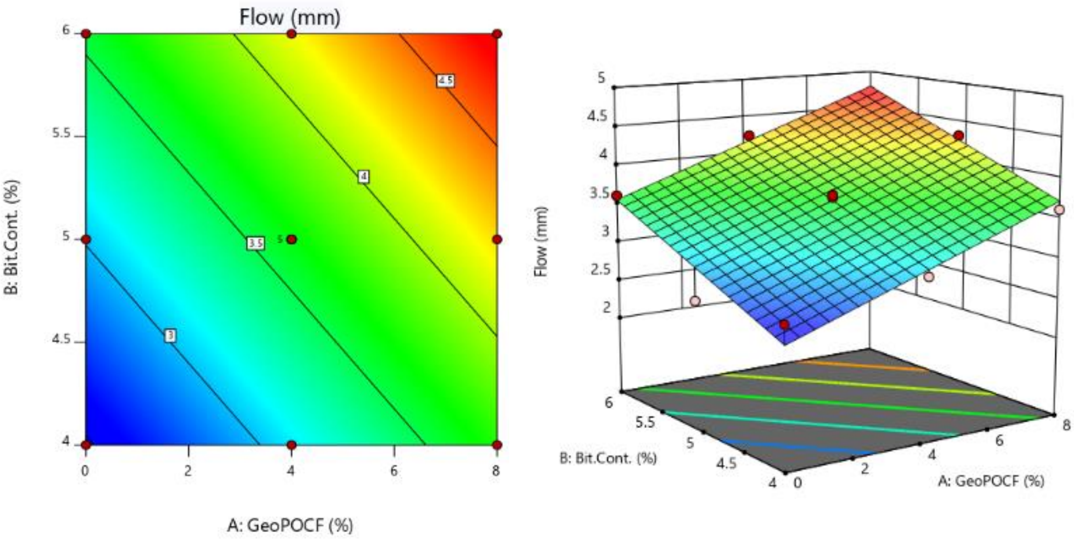


FIGURE 4.6 Effect of GeoPOCF and bitumen contents on Marshall flow (a) 2D (b) 3D

### 4.5 Model Graphs of Perturbation

Perturbation plots in RSM design showed significant parameters by demonstrating variations in response of each component as it progresses away from the reference point, which is the zero coded level of each factor, while all other factors remain constant [28]. The perturbation plot slope also explains the responsiveness of the reaction to changes in each factor [29]. This study assessed the responsiveness of input parameter (GeoPOCF and bitumen content) on output responses (BUW, air voids, Marshall stability and flow).

The perturbation plot for BUW presented in Figure 4.7 revealed that all the two factors significantly influence BUW. However, BUW increases with increased GeoPOCF content (A), while it reduces with increased bitumen content (B). This corroborates that the presence of GeoPOCF contents fills the spaces between the aggregates in compacted modified asphalt mixtures. The highest BUW can be achieved close to the reference point (middle region) of both GeoPOCF content (A) and bitumen content (B).

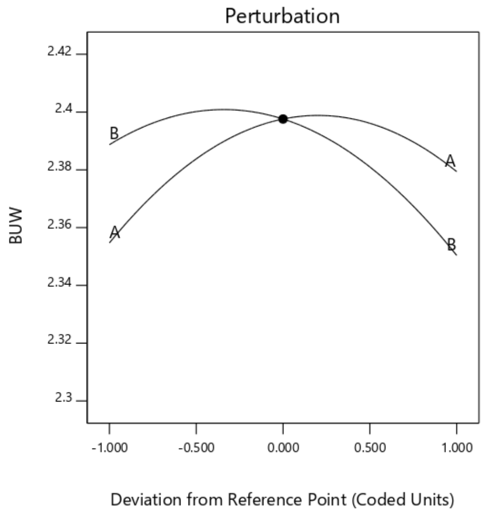


FIGURE 4.7 Perturbation plot for BUW

The perturbation plot for air voids presented in Figure 4.8 revealed that bitumen content had the most significant influence on air voids. The impact of GeoPOCF content (A) was less important when compared to bitumen content (B). The air voids decrease when bitumen content (B) increases. This implies that the increased bitumen content fills the voids of asphalt mixtures.

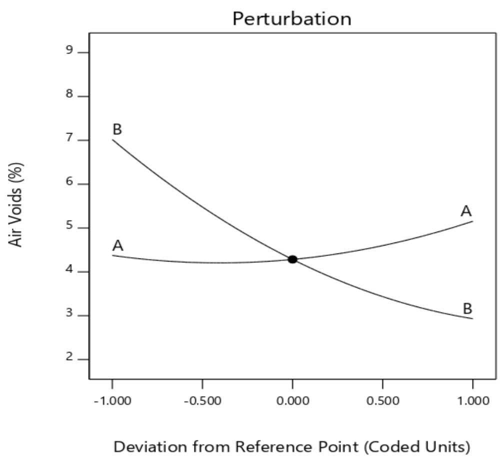


FIGURE 4.8 Perturbation plot for air voids

The perturbation plot for Marshall stability shown in Figure 4.9 demonstrated that the highest Marshall stability could be achieved close to the reference point (middle region) of both GeoPOCF content (A) and bitumen content (B). Furthermore, the steep slope or curvature shows that the Marshall stability is sensitive to the GeoPOCF and bitumen content.

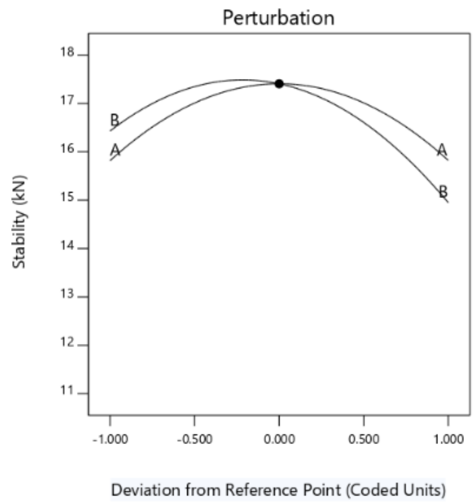


FIGURE 4.9 Perturbation plot for Marshall stability

The perturbation plot for Marshall flow presented in Figure 4.10 showed that all the two factors significantly influence the Marshall flow. The Marshall flow increases with the increase of GeoPOCF content (A) and bitumen content (B).

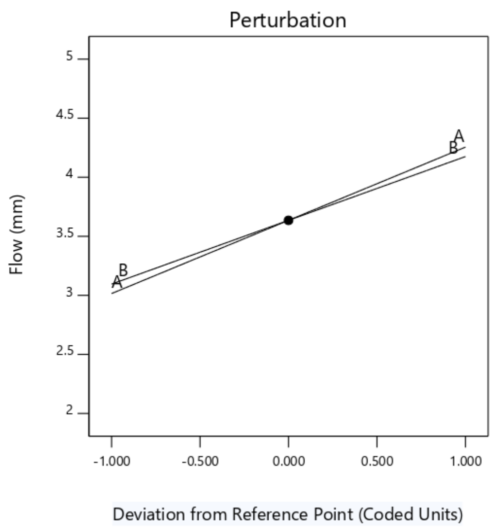


FIGURE 4.10 Perturbation plot for Marshall flow

## 4.6 Numerical Multi-Objective Optimization and Validation of Modeled Results

Numerical optimization was used in this study to find the best independent variable values and the accuracy of the suggested models. Table 4.3 shows the desired goals and optimization ranges, whereas Figure 4.11 shows the optimal values of the independent variables and the maximum predicted responses. With a desirability of 0.849, the optimum GeoPOCF and bitumen concentrations were 6.15% and 4.85%, respectively. The predicted model accuracy was confirmed by repeating the experiment with three replicate samples using the globalized optimum independent parameters derived by numerical optimization analysis and comparing the expected and actual responses.

TABLE 4.3 Selected numerical conditions for optimization for Marshall mix design requirements

| Parameters | Units | Desired goal | Lower Limit | Upper Limit |
|---|---|---|---|---|
| A: GeoPOCF | (%) | maximize | 0 | 8 |
| B: Bit.cont. | (%) | is in range | 4 | 6 |
| BUW | | maximize | 2.313 | 2.409 |
| Air Voids | (%) | is in range | 3 | 5 |
| Marshall Stability | (kN) | maximize | 11.72 | 17.89 |
| Marshall Flow | (mm) | is in range | 2 | 4 |

Table 4.4 shows the validation test results; as a predictability assessment, Equation (6) determines the absolute relative percentage error (RPE) between the laboratory and ideally predicted values. The BUW has the lowest RPE, 1.69%, followed by 3.52% for air voids, 4.57% for Marshall flow, and 4.83% for Marshall stability, as shown in Table 4.4. As an outcome, the models had a high level of accuracy in predicting the responses since the percentage error between the RSM predicted, and laboratory results are < 5% for all responses.

TABLE 4.4 Model validation for laboratory and predicted outputs

| Parameters | BUW | Air Voids | Stability | Flow |
|---|---|---|---|---|
| Units | | (%) | (kN) | (mm) |
| Predicted (RSM) | 2.4 | 5.0 | 17.16 | 3.89 |
| Observed (Laboratory) | 2.36 | 4.83 | 16.37 | 3.72 |
| RPE (%) | 1.69 | 3.52 | 4.83 | 4.57 |
| Remark | Pass | Pass | Pass | Pass |
| Desirability (%) | 84.9 | | | |

$$RPE = \left| 1 - \frac{Predicted\ Values}{Laboratory\ Values} \right| \times 100 \qquad (6)$$

The optimization ramps for GeoPOCF and bitumen contents, as well as desirability value, are shown in Figure 4.11. Every dot on the ramp represents the desired values on input variables and output responses. The desirability of dependent variables ranging from 0 to 1 is revealed on the optimization ramps.

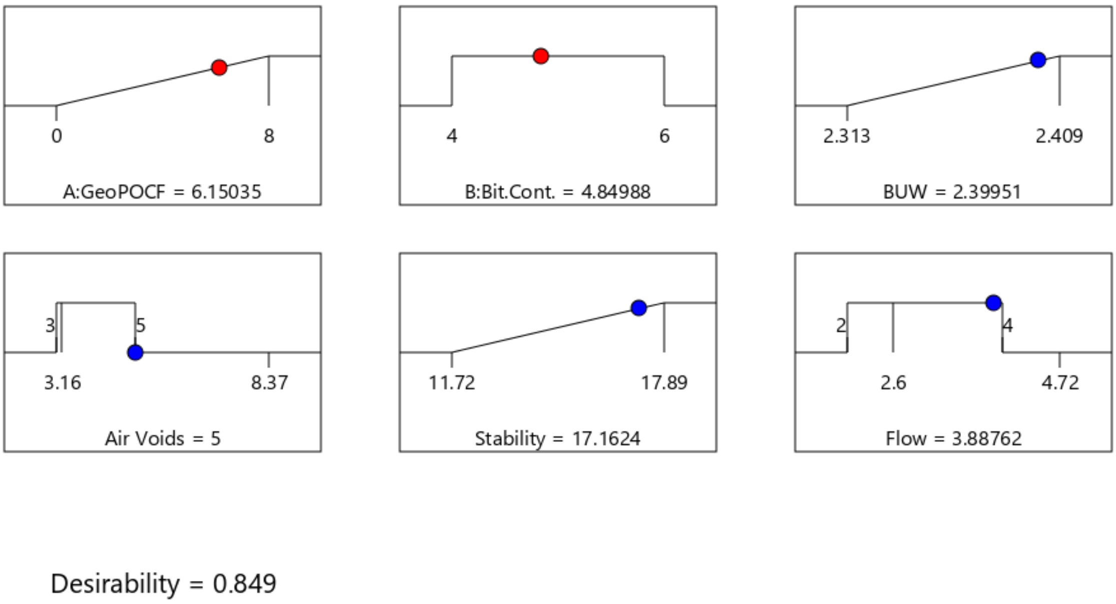


FIGURE 4.11 Numerical optimization ramp for input parameters and output responses

## 4.7 Characterization of GeoPOCF and GeoPOCF modified bitumen

The characterization tests were carried out to better understand the changes that may occur at the microstructural level and the formation of new functional groups as a result of the alteration of bitumen with GeoPOCF. FTIR, XRD, and SEM/EDX were used for the microstructural analysis in this study. In addition, they were utilized to determine the effects of GeoPOCF on the GeoPOCF-MB's rheological characteristics.

### 4.7.1 XRD of GeoPOCF-MB

The XRD technique determines the amount and composition of elements or compounds in a sample. The XRD study of the unmodified bitumen and GeoPOCF-MB was performed using a Panalytical model xpert powder and a Bruker AXS D4 Endeavor diffractometer. It was also used to confirm the crystalline structure of the GeoPOCF-MB samples. The High Score Plus analytical software was used to analyze the XRD results.

To analyze GeoPOCF structure and its presence in bitumen blends, a qualitative XRD was done using diffraction patterns ($2\theta = 5^\circ$-$80^\circ$) with a step of 0.02˚ and exposure period of 10sec/0.02˚ at room temperature. Figure 4.12 shows the XRD patterns of GeoPOCF-MB and unmodified bitumen. The XRD spectrum revealed that the GeoPOCF-MB and unmodified bitumen have quartz-dominated crystalline phases. The existence of the SiO2 structure as the major component of the GeoPOCF is shown by this. The presence of silica in the GeoPOCF is the subject of this research since it may be used to modify bitumen.

The XRD patterns obtained for the unmodified bitumen and GeoPOCF-MB are shown in Figure 4.12. Unmodified bitumen, therefore, has two separate amorphous phases, each with its macromolecular structure. Approximately at 15˚-25˚ and 40˚-45˚ values of $2\theta$, indicating that it formed from crystalline asphaltenes amorphously. The unaltered bitumen sample's XRD traces are similar to those reported in previous studies [3].

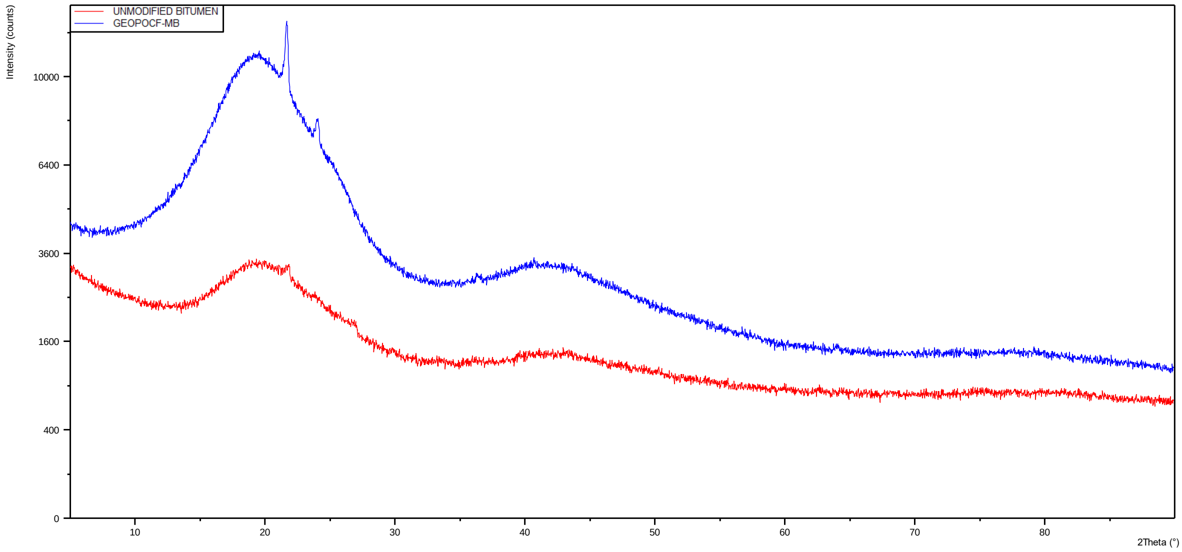


FIGURE 4.12 The XRD patterns of unmodified bitumen and GeoPOCF-MB

Also, the XRD of POCF was previously observed to have references code 01–075-8320, with peaks corresponding to 20.82˚, 26.62˚, and 39.43˚ matchings to planes (100), (011), and (102), respectively, and was compared to the Joint Committee on Powder Diffraction Standards (JCPDS) entry card number 00–46-1045 for silicon oxide/quartz [3]. Therefore, based on the POCF XRD diffraction pattern, the code corresponds to $SiO_2$.

Two significant peaks were found in the XRD of GeoPOCF-MB at 2θ = 21.66˚ (100) and 2θ = 24.02˚ (011), as shown in Figures 4.13 and 4.14, with specific peak values in Tables 4.5 and 4.6. The crystalline structures of the GeoPOCF are fundamental for these peaks. Compared to previous studies, the peaks have shifted to the left, most likely due to the addition of geopolymer to the POCF. Because geopolymer is an inorganic polymer, it needs a fast reaction of silica (Si) and alumina (Al) in an alkaline environment, resulting in a three-dimensional polymeric chain of Si-O-Al-O bonds [18]. The maximum crystallinity and compressive strength level were found in the quartz content of a fly ash-based geopolymer [30]. Therefore, the presence of geopolymer with high crystallinity intensity in this study likely contributed to the high Marshall stability.

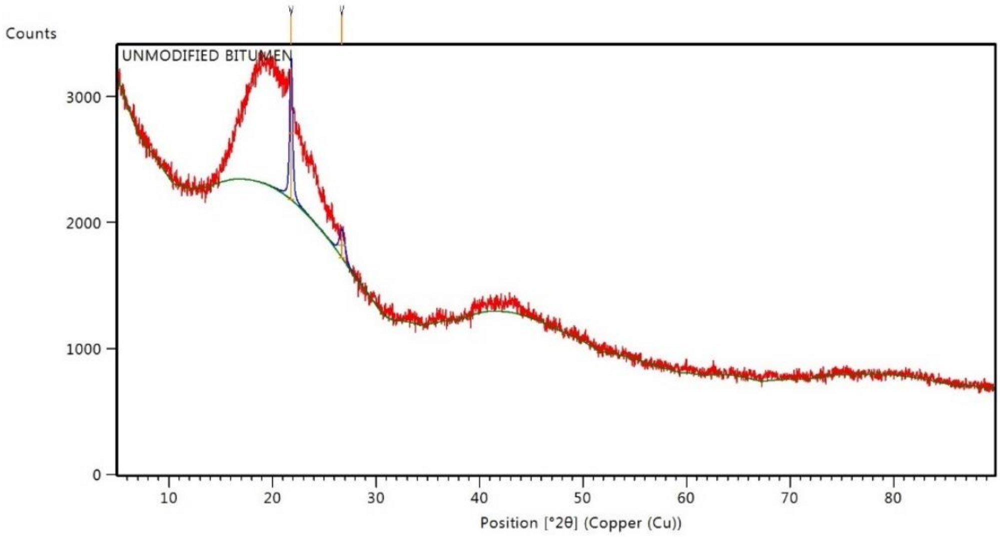


FIGURE 4.13 Peaks produced by XRD analysis for unmodified bitumen

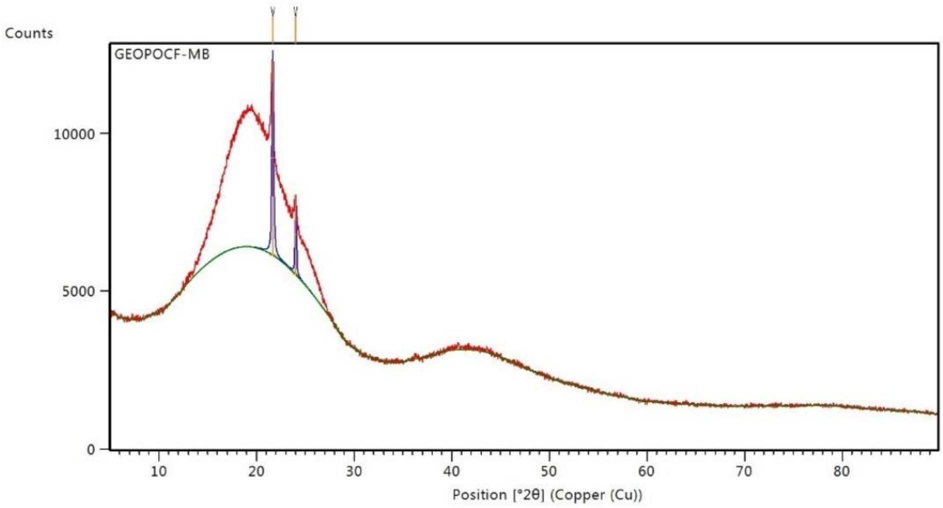


FIGURE 4.14 Peaks produced by XRD analysis for unmodified bitumen

Table 4.5 GeoPOCF-MB XRD results

| **Peak** | **2-Theta (θ) degree** | **d-spacing (nm)** |
|---|---|---|
| 1 | 21.66 | 4.102 |
| 2 | 24.02 | 3.706 |

TABLE 4.6 Unmodified bitumen XRD results

| **Peak** | **2-Theta (θ) degree** | **d-spacing (nm)** |
|---|---|---|
| 1 | 21.8 | 4.077 |
| 2 | 26.73 | 3.335 |

### 4.7.2 FTIR of GeoPOCF-MB

The functionality formation and possible interaction between the bitumen and GeoPOCF were investigated using FTIR characterization. On a range of 500 to 4000 $cm^{-1}$, FT-IR spectra were observed. The infrared spectra (IR) of the GeoPOCF powder are shown in Figure 4.15. The study reveals essential details regarding functional groups and their relationships with other functional groups. FTIR readings were also used to identify the quartz and cristobalite minerals in GeoPOCF.

In FTIR spectra, the peak for organic carbon is about 3000 $cm^{-1}$. One of the essential minerals in POCF is quartz, which is almost always present. The existence of two bands at 1000 and 1080 $cm^{-1}$, generated by vibrations in the stretching and bending bands of (Si-O) in SiO4, shows crystalline components in the samples, such as quartz grains. Si-O-Si vibration bending resulted in peaks ranging from 469 to 619 $cm^{-1}$. Furthermore, 3434 $cm^{-1}$ represents the vibrations of O-H stretching and H-O-H bending [3]. In comparison to the previous analysis, there is an increased occurrence of bands from 795 to 850 $cm^{-1}$, indicating a geopolymer element's existence.

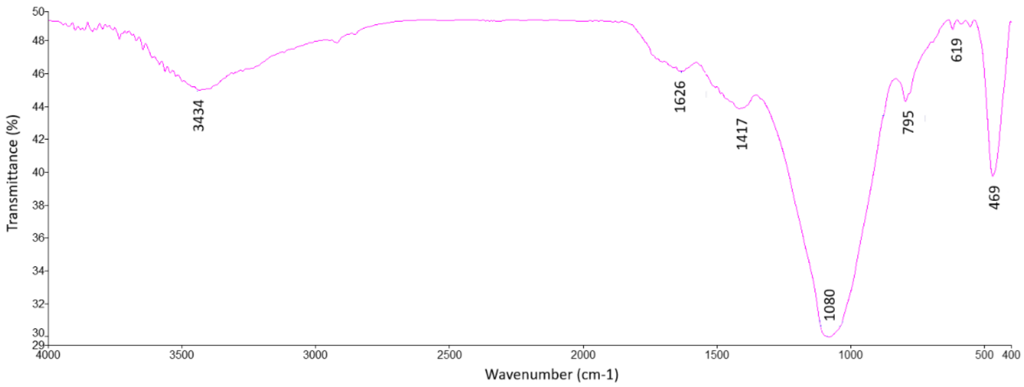


FIGURE 4.15 FTIR spectra of GeoPOCF

Figure 4.16 illustrates the phase peak intensities of GeoPOCF powder, unmodified bitumen, and GeoPOCF-MB in the infrared bitumen spectrum. Around wavenumbers of 1000 to 1500 $cm^{-1}$, using GeoPOCF-MB capabilities had a considerable influence. $Si(OH)_4$ was suggested by an absorption band of roughly 1010 $cm^{-1}$, which corresponds typically to Si-O-Si stretch vibrations caused by the deformation of Si-O bonds, indicating that silica is broadly reactive to bitumen [3]. The prominent bands found for unmodified bitumen differ slightly from the GeoPOCF-MB, it was discovered. The addition of GeoPOCF is thought to improve the performance of asphalt mixes.

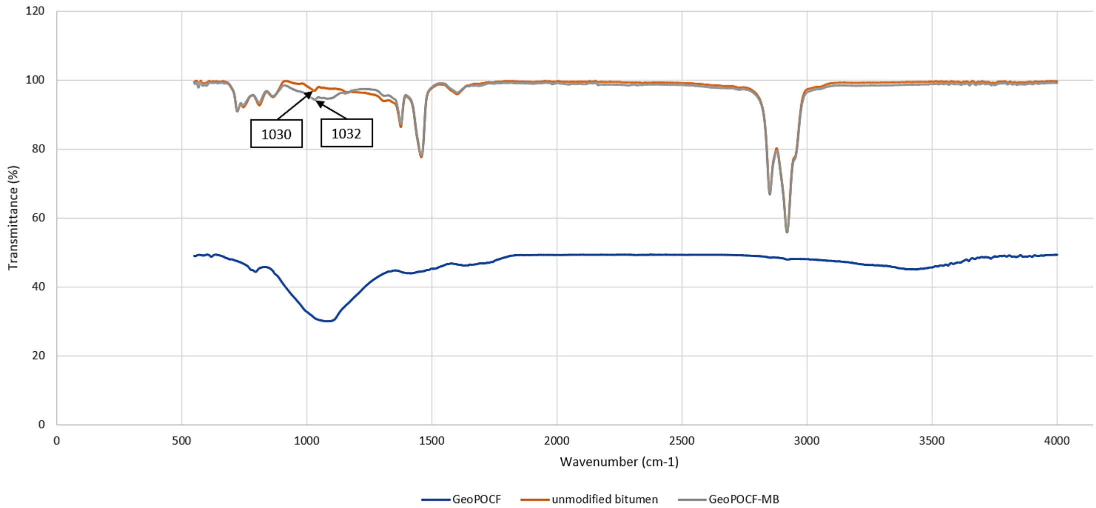


FIGURE 4.16 Combined FTIR spectra of GeoPOCF powder, unmodified bitumen and GeoPOCF-MB

### 4.7.3 SEM/EDX of GeoPOCF-MB

The surface morphology of the unmodified bitumen and changes in the surface morphology of the GeoPOCF-MB were analyzed using SEM. SEM/EDX analysis was performed using a scanning electron microscope with ultrahigh-resolution (SUPRA 55VP by Carl Zeiss model, EVO LS15 Germany).

As shown in Table 4.7, the relative percentages of each element were computed on a chosen specific area of the unmodified bitumen and GeoPOCF-MB surface and conducted an EDX analysis of each component inside the defined area on its surface. The primary elements were oxygen, carbon, silicon, sodium, sulfur, magnesium, and aluminum, according to the EDX. These data show that GeoPOCF possesses pozzolanic characteristics.

TABLE 4.7 Quantity analysis from EDX on unmodified bitumen and GeoPOCF-MB

| | **Unmodified bitumen** | | **GeoPOCF-MB** | |
|---|---|---|---|---|
| **Element** | **Atomic (%)** | **Weight (%)** | **Atomic (%)** | **Weight (%)** |
| Aluminum | 0.01 | 0.03 | 0.07 | 0.15 |
| Calcium | 0.00 | 0.01 | 0.00 | 0.01 |
| Carbon | 94.92 | 91.82 | 93.34 | 90.14 |
| Magnesium | 0.01 | 0.01 | 0.02 | 0.04 |
| Oxygen | 3.83 | 4.93 | 5.58 | 7.17 |
| Silicon | 0.00 | 0.01 | 0.11 | 0.24 |
| Sodium | 0.01 | 0.03 | 0.05 | 0.10 |
| Sulfur | 1.19 | 3.07 | 0.83 | 2.14 |
| Zinc | 0.02 | 0.09 | 0.00 | 0.01 |

Electron micrographs of the unmodified bitumen droplet and the GeoPOCF-MB are shown in Figures 4.17 and 4.18. As a result of the effective integration of GeoPOCF into the bitumen, it was noticed that the GeoPOCF was equally spread. The SEM picture of unmodified bitumen reveals that its composition is in a homogenous phase. The GeoPOCF particles were dispersed in the modified sample, indicating that it had been considerably transformed compared to the original bitumen. However, it is different from previous work. Small particles were absent in the POCF-MB. As shown in Figure 4.18, adding geopolymer results in unreacted small particles. GeoPOCF particles were what these particles were called. In a previous study, unreacted geopolymer material was detected, and these unreacted particles reduced the compressive strength of the geopolymer structure [19]. The geopolymer binder was also found to have microcracks [25].

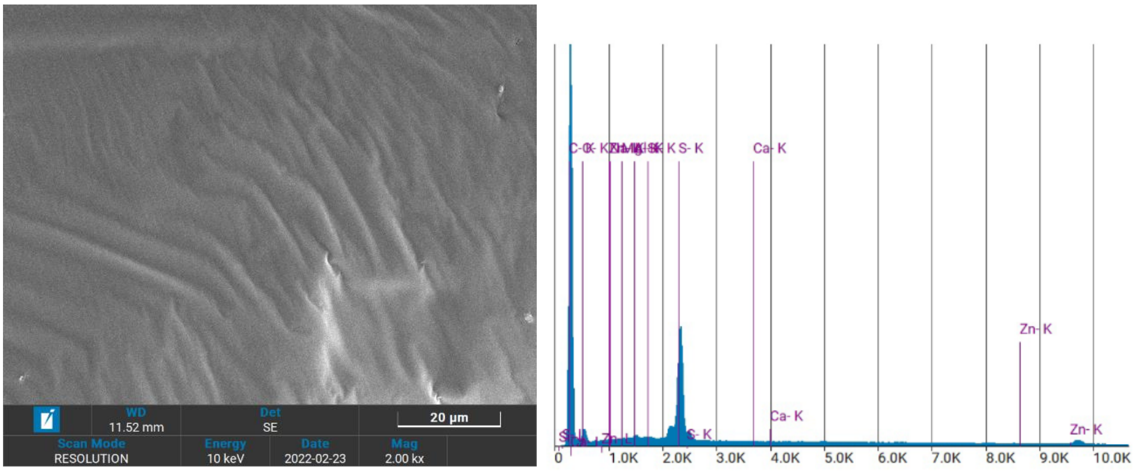


FIGURE 4.17 SEM images and EDX of unmodified bitumen

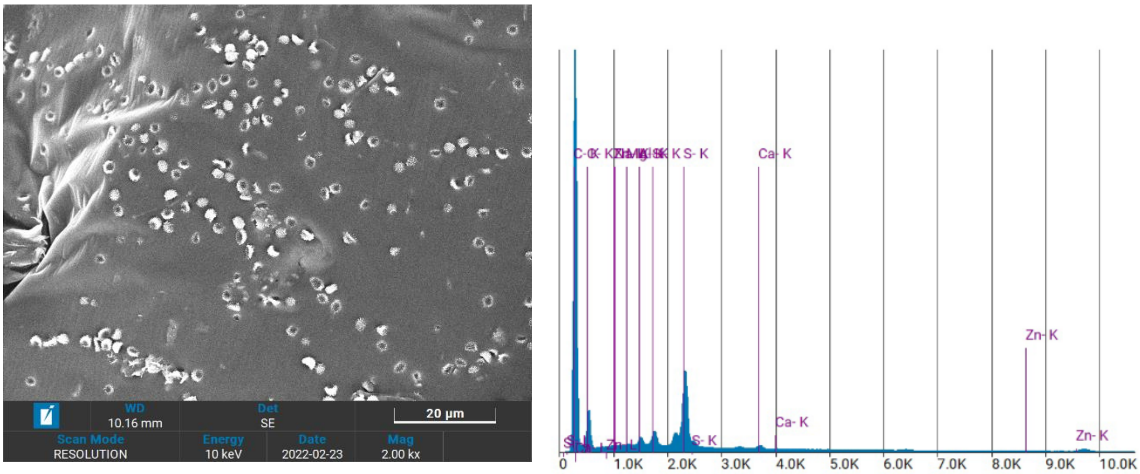


FIGURE 4.18 SEM images and EDX of GeoPOCF-MB

# CHAPTER 5

## CONCLUSION

In conclusion, the objectives of this research study have been achieved. The optimization of GeoPOCF and bitumen content and models on the effect of GeoPOCF modified bitumen on asphalt mixtures volumetric and Marshall parameters successfully obtained using RSM software and laboratory works, the optimum GeoPOCF and bitumen content were 6.15%, and 4.85%, respectively. Furthermore, the study findings were reliable since the percentage error between the RSM predicted, and laboratory results are $< 5\%$ for all responses when using the optimum GeoPOCF and bitumen content. Besides, the GeoPOCF, unmodified bitumen and GeoPOCF modified bitumen at optimized content were successfully characterized using XRD, FTIR, and SEM analysis. The analysis shows the great potential of using GeoPOCF as an alternative bitumen modifier. Therefore, this project is beneficial to be conducted as an innovative study on industrial-waste materials used in asphalt mixtures where it increases pavement performance.

## RECOMMENDATION

1. It is recommended to conduct a study on X-ray Fluorescence (XRF) analysis to examine the chemical compositions in GeoPOCF.
2. It is recommended that other mechanical performance tests should be carried out.
3. Rheological analysis using a dynamic shear rheometer (DSR) should be conducted to properly understand modified bitumen behavior's viscoelastic behavior.

# REFERENCES


[1] R. Dungani *et al.*, "Biomaterial from Oil Palm Waste: Properties, Characterization and Applications," in *Palm Oil*, 2018, ch. Chapter 3.

[2] S. Mabroum, S. Moukannaa, A. El Machi, Y. Taha, M. Benzaazoua, and R. Hakkou, "Mine wastes based geopolymers: A critical review," *Cleaner Engineering and Technology,* vol. 1, 2020, doi: 10.1016/j.clet.2020.100014.

[3] N. S. A. Yaro, M. B. Napiah, M. H. Sutanto, A. Usman, and S. M. Saeed, "Modeling and optimization of mixing parameters using response surface methodology and characterization of palm oil clinker fine modified bitumen," *Construction and Building Materials,* Article vol. 298, 2021, Art no. 123849, doi: 10.1016/j.conbuildmat.2021.123849.

[4] D. Zhao *et al.*, "High industrial solid waste road base course binder: Performance regulation, hydration characteristics and practical application," *Journal of Cleaner Production,* vol. 313, 2021, doi: 10.1016/j.jclepro.2021.127879.

[5] A. Mohammed Babalghaith, S. Koting, N. H. Ramli Sulong, M. R. Karim, and B. Mohammed AlMashjary, "Performance evaluation of stone mastic asphalt (SMA) mixtures with palm oil clinker (POC) as fine aggregate replacement," *Construction and Building Materials,* vol. 262, p. 120546, 2020/11/30/ 2020, doi: https://doi.org/10.1016/j.conbuildmat.2020.120546.

[6] W. Rafiq *et al.*, "Modeling and design optimization of reclaimed asphalt pavement containing crude palm oil using response surface methodology," *Construction and Building Materials,* Article vol. 291, 2021, Art no. 123288, doi: 10.1016/j.conbuildmat.2021.123288.

[7] M. Nawaz, A. Heitor, and M. Sivakumar, "Geopolymers in construction - recent developments," *Construction and Building Materials,* vol. 260, p. 120472, 2020/11/10/ 2020, doi: https://doi.org/10.1016/j.conbuildmat.2020.120472.

[8] A. Hamid, H. Alfaidi, H. Baaj, and M. El-Hakim, "Evaluating Fly Ash-Based Geopolymers as a Modifier for Asphalt Binders," *Advances in Materials Science and Engineering,* vol. 2020, pp. 1-11, 2020, doi: 10.1155/2020/2398693.

[9] M. R. Mohd Hasan, J. W. Chew, A. Jamshidi, X. Yang, and M. O. Hamzah, "Review of sustainability, pretreatment, and engineering considerations of asphalt modifiers from the industrial solid wastes," *Journal of Traffic and Transportation Engineering (English Edition),* vol. 6, no. 3, pp. 209-244, 2019/06/01/ 2019, doi: https://doi.org/10.1016/j.jtte.2018.08.001.

[10] S. A. R. Shah *et al.*, "Marshall stability and flow analysis of asphalt concrete under progressive temperature conditions: An application of advance decision-making approach," *Construction and Building Materials,* vol. 262, 2020, doi: 10.1016/j.conbuildmat.2020.120756.

[11] Y. Zhang, H. Cheng, L. Sun, L. Liu, and Y. Hu, "Determination of volumetric criteria for designing hard asphalt mixture," *Construction and Building Materials,* vol. 278, 2021, doi: 10.1016/j.conbuildmat.2021.122243.

[12] J. Zhu, X. Lu, and N. Kringos, "Experimental investigation on storage stability and phase separation behaviour of polymer-modified bitumen," *International Journal of Pavement Engineering,* vol. 19, no. 9, pp. 832-841, 2018/09/02 2018, doi: 10.1080/10298436.2016.1211870.

[13] A. ASTM, "D6927-15 Standard Test Method for Marshall Stability and Flow of Asphalt Mixtures," *ASTM International: West Conshohocken, PA, USA, ,* 2015, doi: 10.1520/d6927-15.
[14] A. Malaysia, "Standard Specification for Road Works, Section 4, Flexible Pavement, Jabatan, Kerja Raya Malaysia, Kuala Lumpur," 2008.
[15] B. N. Akshitha, M. S. Balreddy, and S. Sunil, "Laboratory investigation of stone mastic asphalt using reclaimed asphalt pavement," *Materials Today: Proceedings*, 2022, doi: 10.1016/j.matpr.2022.02.274.
[16] B. Singh Sidhu, M. Singh, and J. Singh, "Investigation on limestone and granite as aggregates in bituminous concrete prepared using ETA and PPA modified bitumen," *Materials Today: Proceedings*, vol. 48, pp. 1253-1257, 2022, doi: 10.1016/j.matpr.2021.08.264.
[17] D. Baş and İ. H. Boyacı, "Modeling and optimization I: Usability of response surface methodology," *Journal of Food Engineering*, vol. 78, no. 3, pp. 836-845, 2007/02/01/ 2007, doi: https://doi.org/10.1016/j.jfoodeng.2005.11.024.
[18] C.-K. Ma, A. Z. Awang, and W. Omar, "Structural and material performance of geopolymer concrete: A review," *Construction and Building Materials*, vol. 186, pp. 90-102, 2018, doi: 10.1016/j.conbuildmat.2018.07.111.
[19] E. Pawluczuk, K. Kalinowska-Wichrowska, J. R. Jiménez, J. M. Fernández-Rodríguez, and D. Suescum-Morales, "Geopolymer concrete with treated recycled aggregates: Macro and microstructural behavior," *Journal of Building Engineering*, vol. 44, 2021, doi: 10.1016/j.jobe.2021.103317.
[20] N. S. A. Yaro, M. Napiah, M. H. Sutanto, A. Usman, S. M. Saeed, and J. M. Kaura, "Influence of modification mixing parameters on conventional properties of palm oil clinker fine (POCF)-modified bitumen," *Materials Today: Proceedings*, vol. 48, pp. 771-777, 2022, doi: 10.1016/j.matpr.2021.02.250.
[21] N. S. A. Yaro, M. H. Sutanto, N. Z. Habib, M. Napiah, A. Usman, and A. Muhammad, "Comparison of Response Surface Methodology and Artificial Neural Network approach in predicting the performance and properties of palm oil clinker fine modified asphalt mixtures," *Construction and Building Materials*, vol. 324, 2022, doi: 10.1016/j.conbuildmat.2022.126618.
[22] S. Sembiring, "Bituminous Composite Comprising Amorphous Silica from Rice Husks," *Ceramics - Silikaty*, pp. 277-286, 2019, doi: 10.13168/cs.2019.0021.
[23] F. Wang, Y. Xiao, Z. Chen, P. Cui, J. Liu, and N. Wang, "Morphological characteristics of mineral filler and their influence on active adhesion between aggregates and bitumen," *Construction and Building Materials*, vol. 323, 2022, doi: 10.1016/j.conbuildmat.2022.126520.
[24] S. N. A. Razak, N. Shafiq, L. Guillaumat, S. A. Farhan, and V. K. Lohana, "Fire-Exposed Fly-Ash-Based Geopolymer Concrete: Effects of Burning Temperature on Mechanical and Microstructural Properties," *Materials (Basel)*, vol. 15, no. 5, Mar 3 2022, doi: 10.3390/ma15051884.
[25] K. Sun, X. Peng, S. H. Chu, S. Wang, L. Zeng, and G. Ji, "Utilization of BOF steel slag aggregate in metakaolin-based geopolymer," *Construction and Building Materials*, vol. 300, 2021, doi: 10.1016/j.conbuildmat.2021.124024.
[26] A. Usman, M. H. Sutanto, M. Napiah, S. E. Zoorob, S. Abdulrahman, and S. M. Saeed, "Irradiated polyethylene terephthalate fiber and binder contents optimization for fiber-reinforced asphalt mix using response surface

methodology," *Ain Shams Engineering Journal*, vol. 12, no. 1, pp. 271-282, 2021, doi: 10.1016/j.asej.2020.06.011.

[27] B. S. Mohammed, S. Haruna, M. Mubarak bn Abdul Wahab, and M. S. Liew, "Optimization and characterization of cast in-situ alkali-activated pastes by response surface methodology," *Construction and Building Materials*, vol. 225, pp. 776-787, 2019, doi: 10.1016/j.conbuildmat.2019.07.267.

[28] T. F. Awolusi, O. L. Oke, O. O. Akinkurolere, and A. O. Sojobi, "Application of response surface methodology: Predicting and optimizing the properties of concrete containing steel fibre extracted from waste tires with limestone powder as filler," *Case Studies in Construction Materials*, vol. 10, 2019, doi: 10.1016/j.cscm.2018.e00212.

[29] O. Rejeb *et al.*, "Parametric analysis and new performance correlation of the surface conventional rigid pavement temperature," *Case Studies in Construction Materials*, vol. 16, 2022, doi: 10.1016/j.cscm.2022.e00923.

[30] A. R. Alvee *et al.*, "Experimental study of the mechanical properties and microstructure of geopolymer paste containing nano-silica from agricultural waste and crystalline admixtures," *Case Studies in Construction Materials*, vol. 16, 2022, doi: 10.1016/j.cscm.2021.e00792.